Predictions of the onset of Flow Instabilities and Gross Surface Irregularities of Energetic Grains During Extrusion

Joint Ordnance Commanders Group (JOCG)
Continuous Mixer & Extruder Users Group (CMEUG)
13-14 October 2004

D. M. Kalyon, H. Tang, E. Birinci, H. Gevgilili
Stevens Institute of Technology

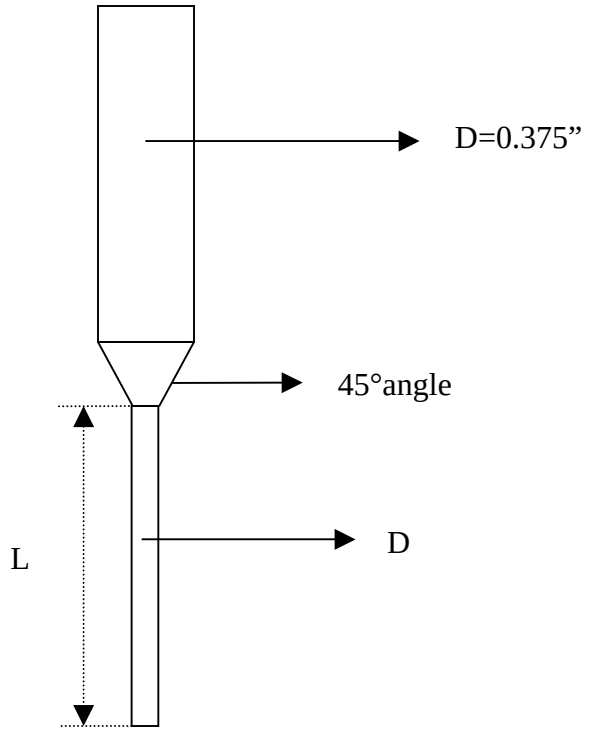

Flow through a simple capillary die (Poiseuille flow).

PDMS

45deg d=0.096 L/D=40 Crosshead Speed: 2in/min

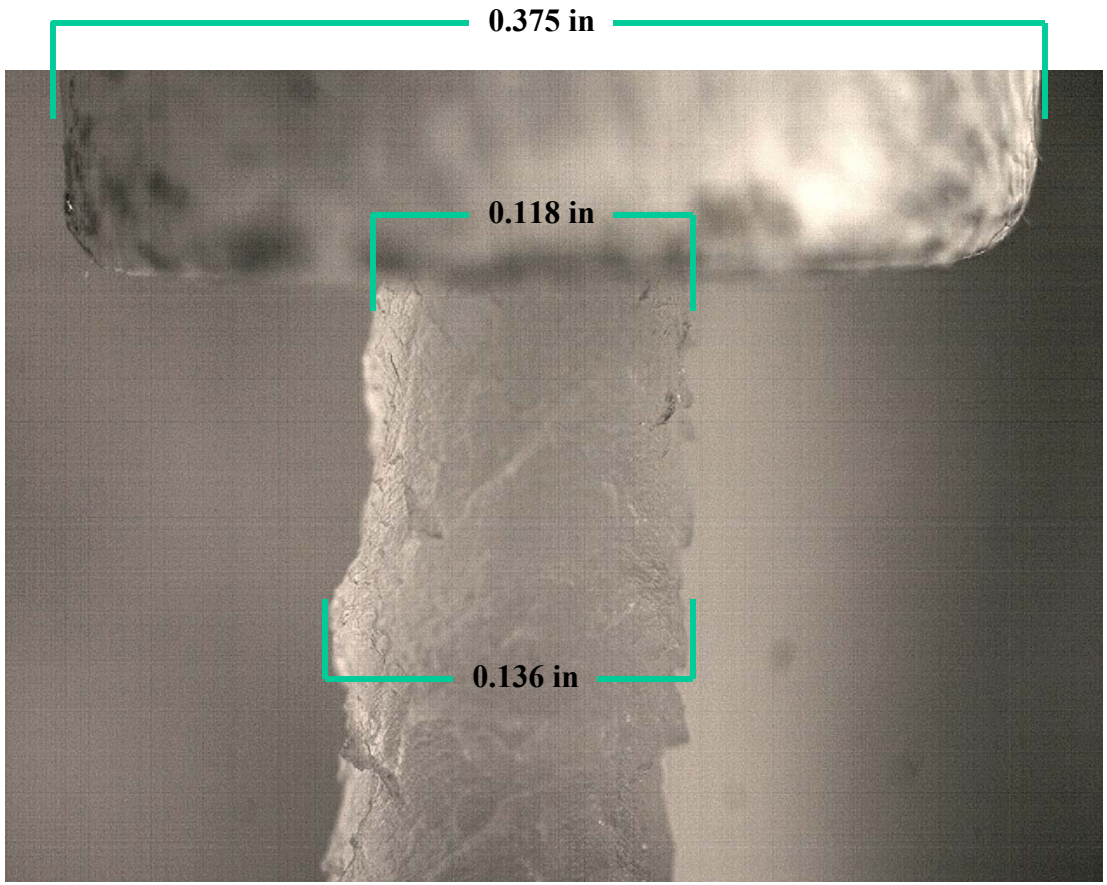

Thermal Imaging Camera

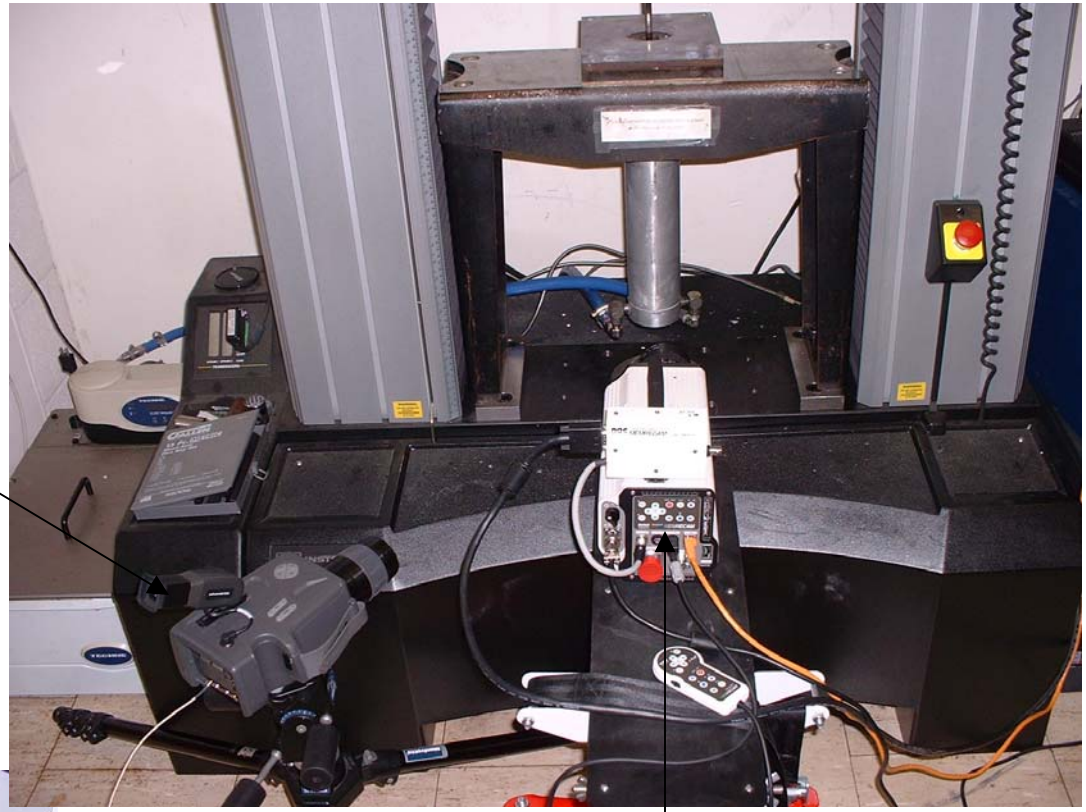

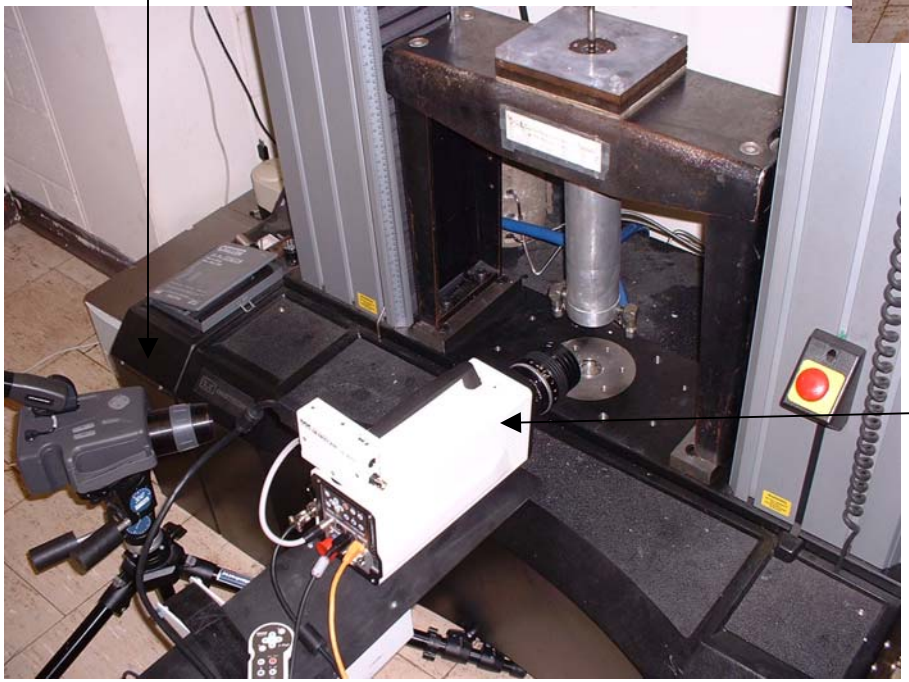

High Speed Camera

PDMS Gross melt fract d=0.096 LD40

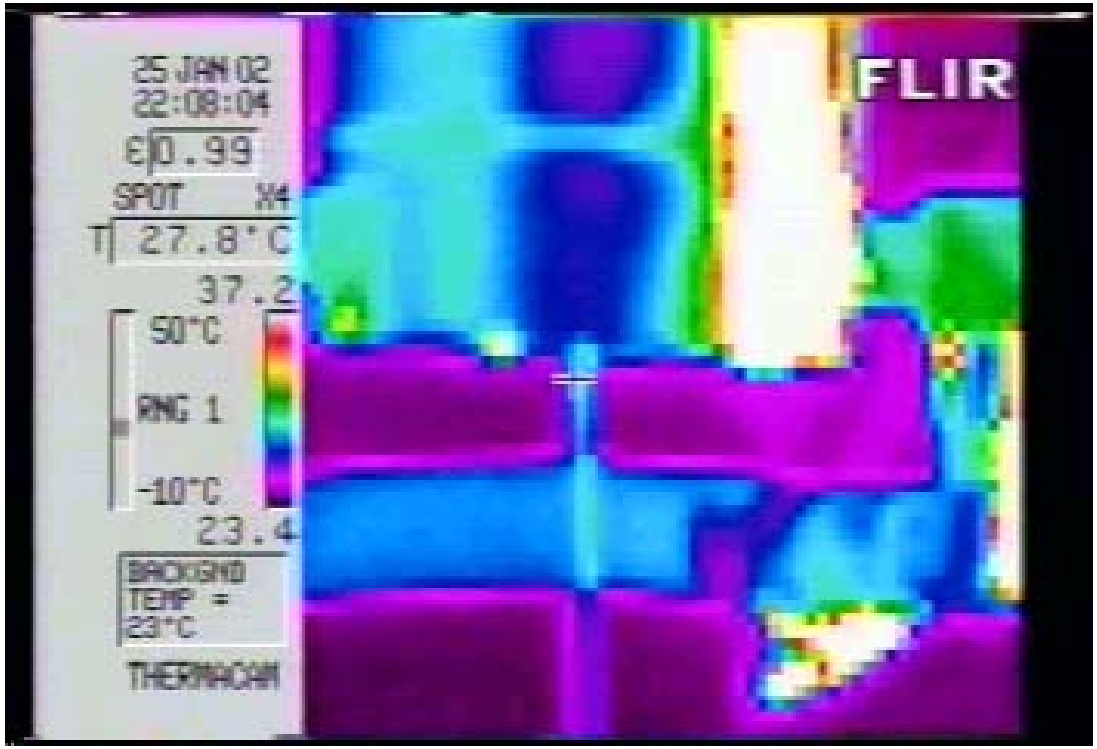

Thermal video of the capillary extrusion of PDMS

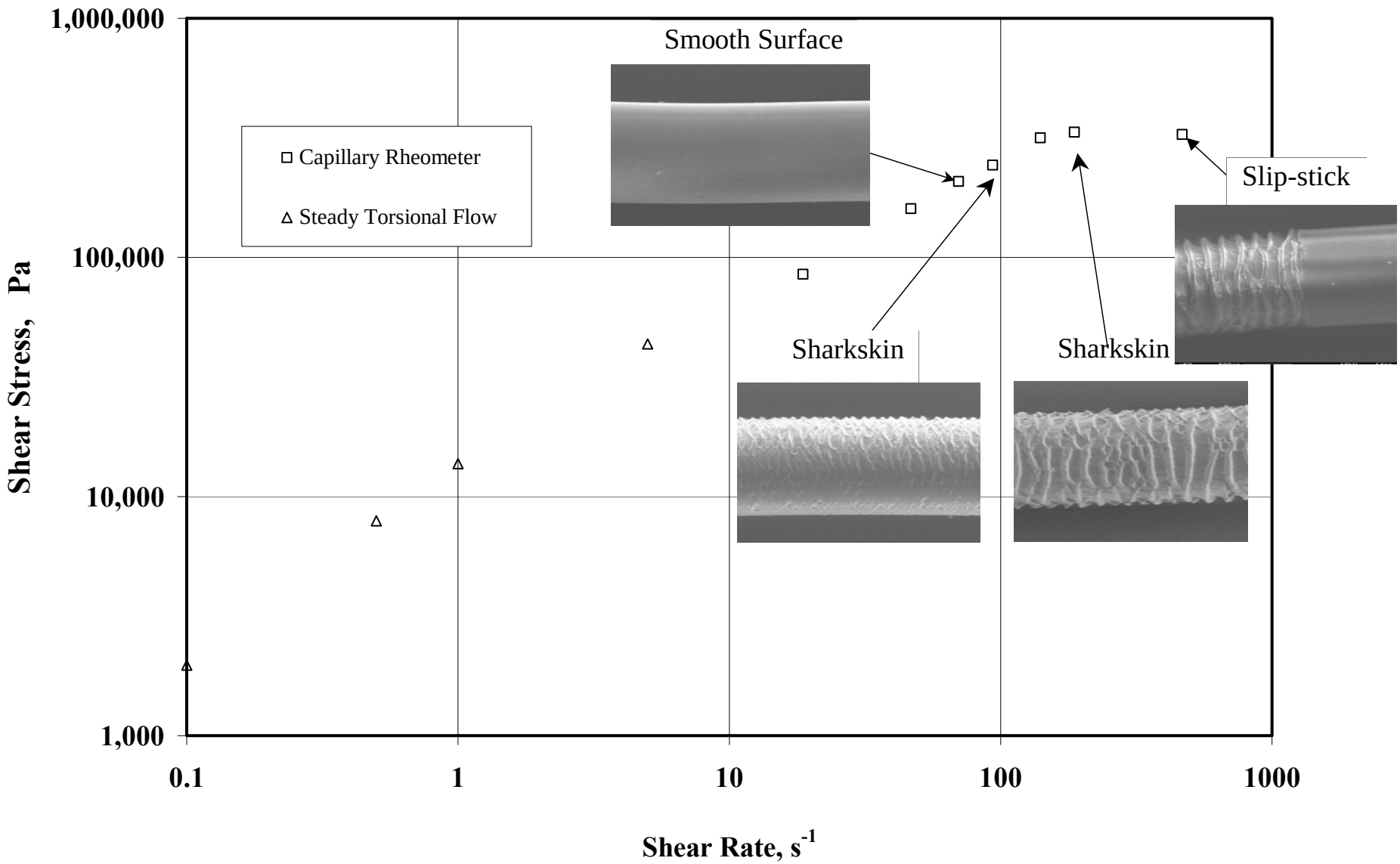

HDPE in capillary flow, development of surface irregularities

Experimental investigation

- PDMS, HDPE, BAMO/AMMO-TPE wall slip behavior in steady torsional flow and development of surface irregularities in capillary flow
- Filled PDMS 10,20,40% by volume hollow glass spheres and KCl Filled BAMO/AMMO- TPE.

Important points

- Materials which do exhibit strong slip exhibit flow instabilities during extrusion commencing at the shear stress at which strong slip is observed. Incorporation of rigid particles at the right concentration eliminates all types of surface irregularities during extrusion.
- Melt which does not exhibit strong slip for relatively high strains and shear rates does not exhibit surface irregularities in the same shear rate range. However, the incorporation of rigid particles introduces surface irregularities during extrusion.

Conclusion

It appears that the stability of stick or slip at the wall during extrusion governs the occurrence of surface irregularities.

Through mathematical modeling we aim to understand the formation mechanisms of flow instabilities which present bottlenecks to production rates.

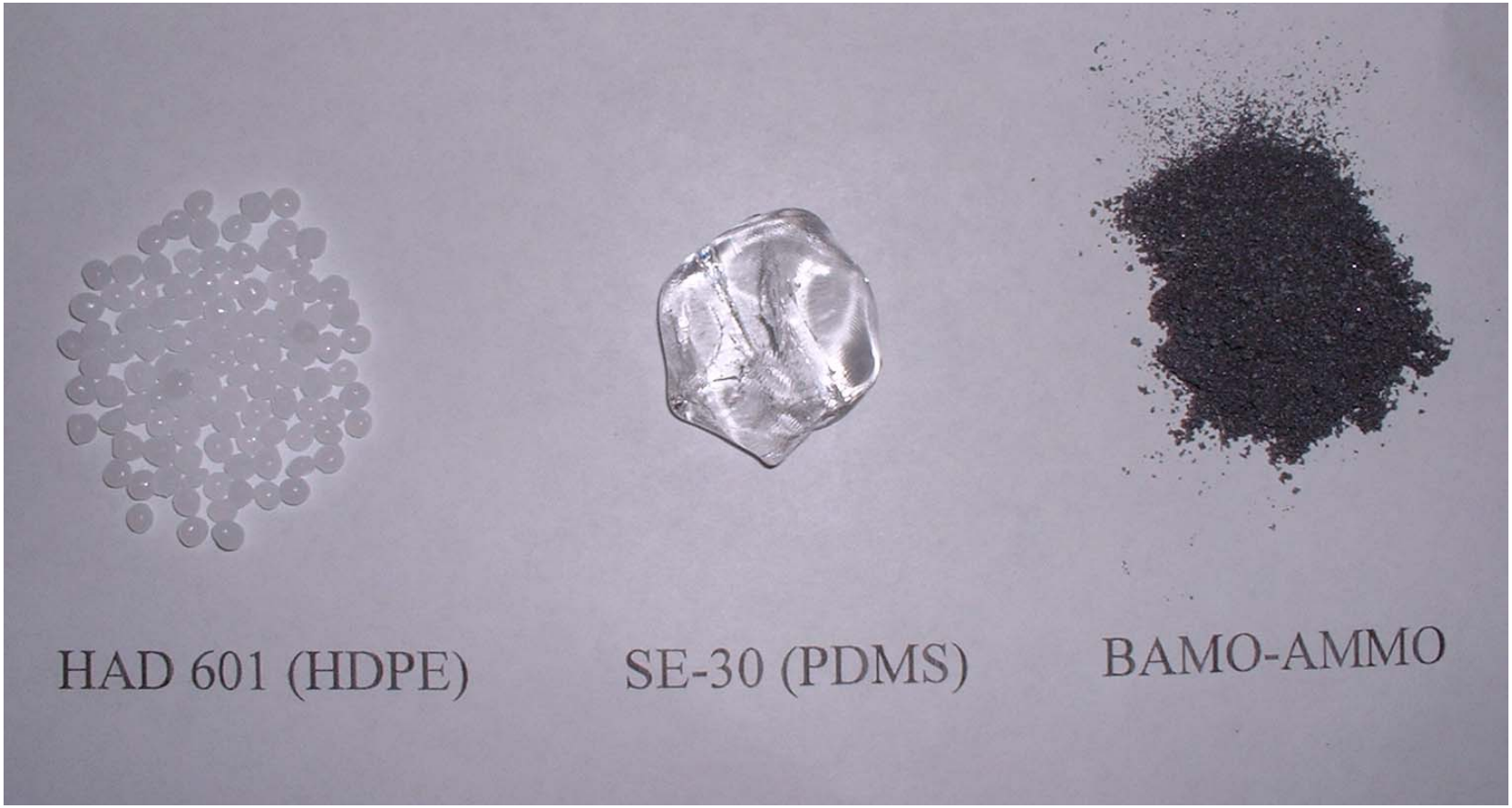
HAD 601 (HDPE)
SE-30 (PDMS)
BAMO-AMMO

- HAD 601 high density polyethylene available from Exxon-Mobil Chemical Company

  Melt flow index=0.55 (according to ASTM D-1238)

  Density=0.933 g/cm^3 (according to ASTM D-1505)

- Polydimethylsiloxane (PDMS SE-30) manufactured by GE Silicones

  Density=0.98 g/cm^3 at 30°C

- A Thermoplastic Elastomer: BAMO-AMMO available from Thiokol Propulsion Corporation

Structure of BAMO-AMMO

BAMO bis(3-azidomethlyene) oxetane

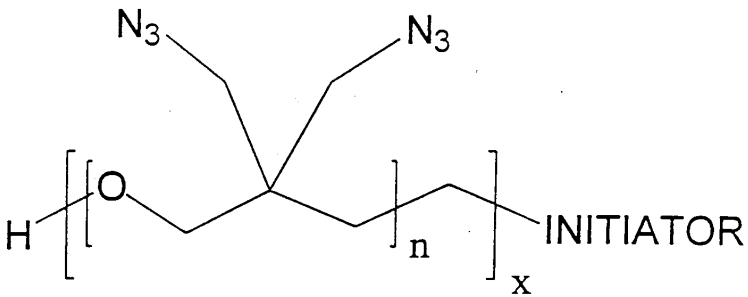

AMMO 3-azidomethlyene-3-methyl oxetane

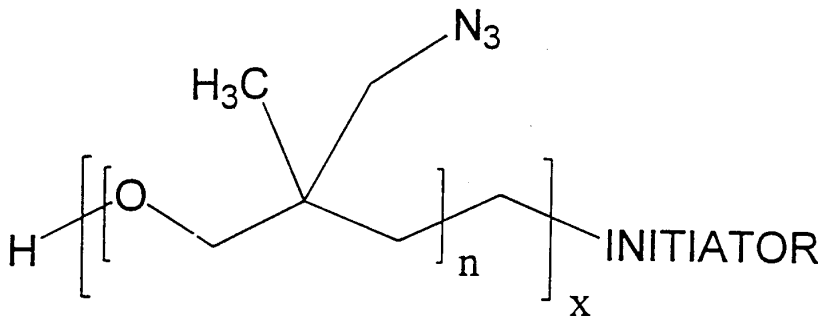

Consisting of of 3, 3-bis (azidomethyl) oxetane, BAMO, which is a crystalline homopolymer and the soft block consisting of 3-azidometyl-3-metyloxetane, AMMO, which is an amorphous homopolymer, forming the soft block of this energetic thermoplastic elastomer

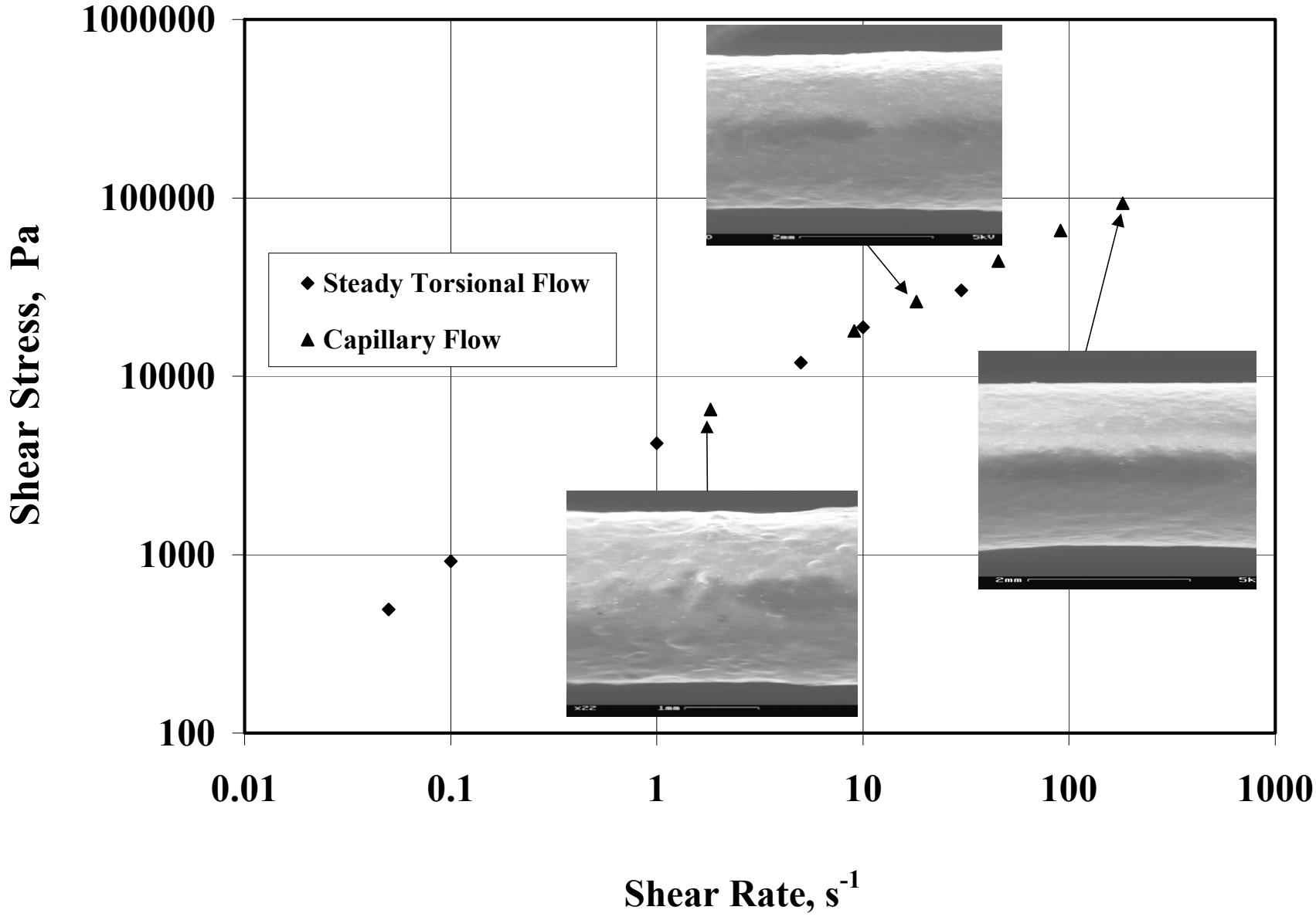

BAMO/AMMO TPE no surface irregularities

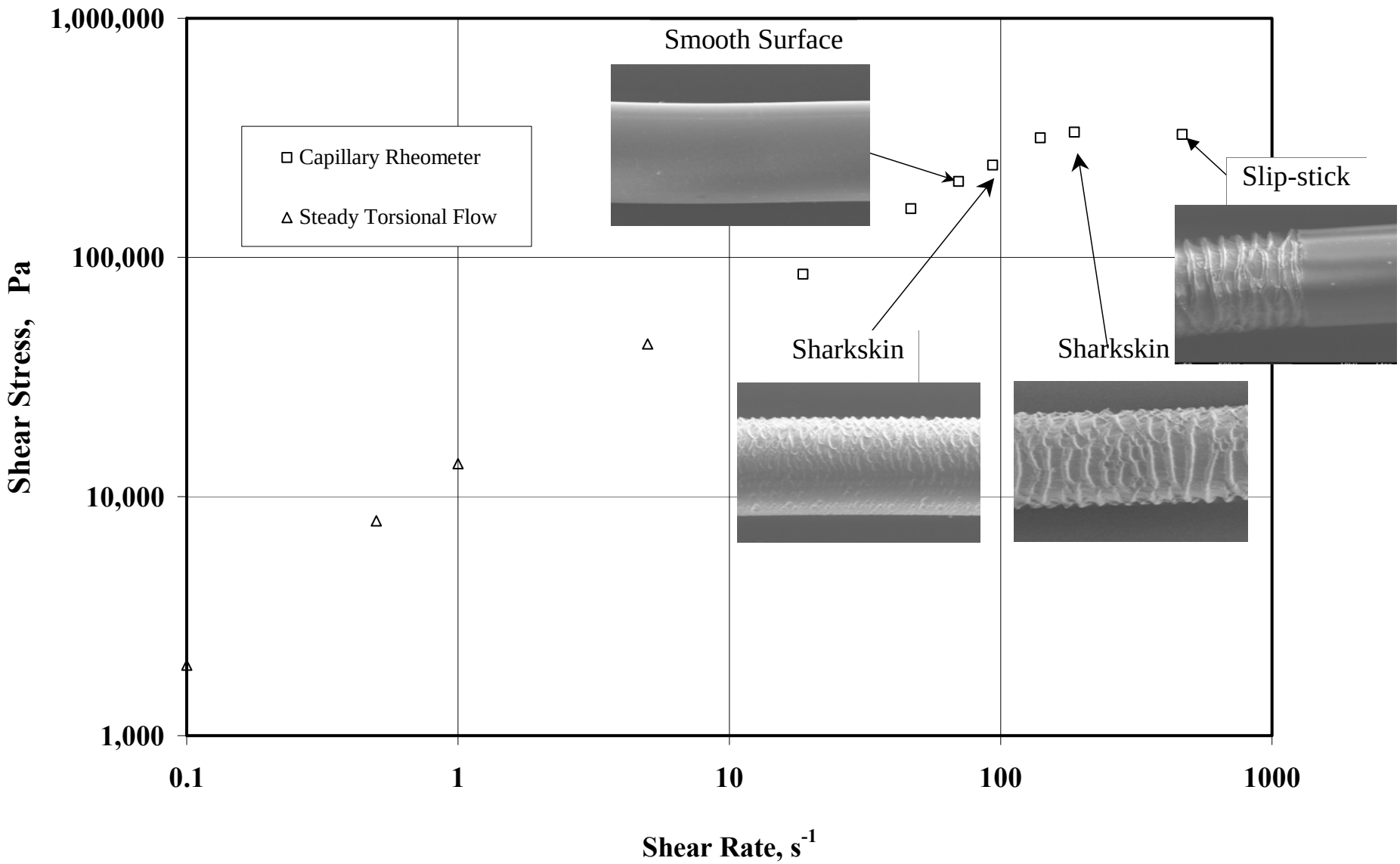

HDPE in capillary flow, development of surface irregularities

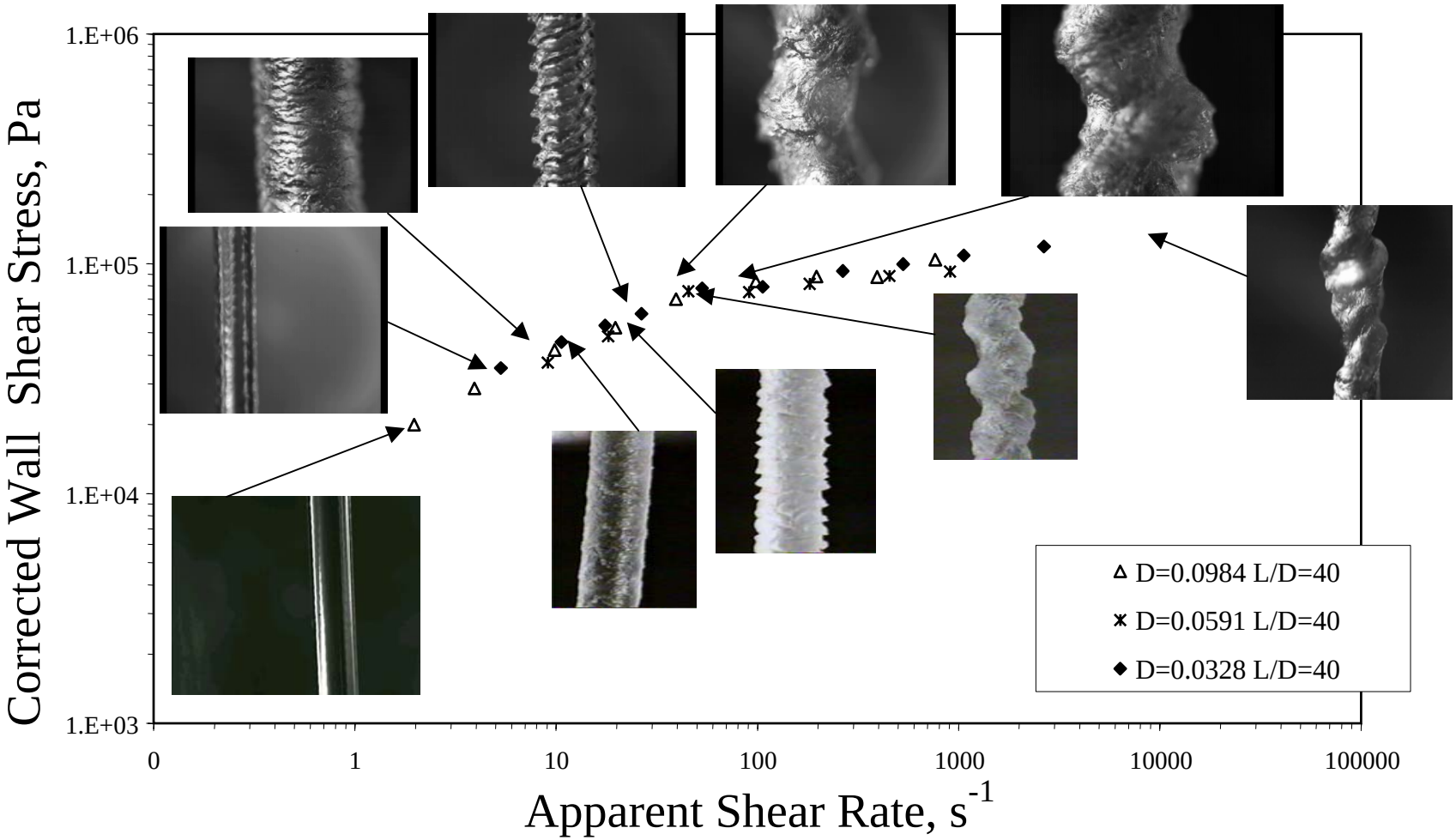

Flow curves and extrudates of poly(dimethyl siloxane) collected with capillaries with different diameters and development of extrudate surface irregularities

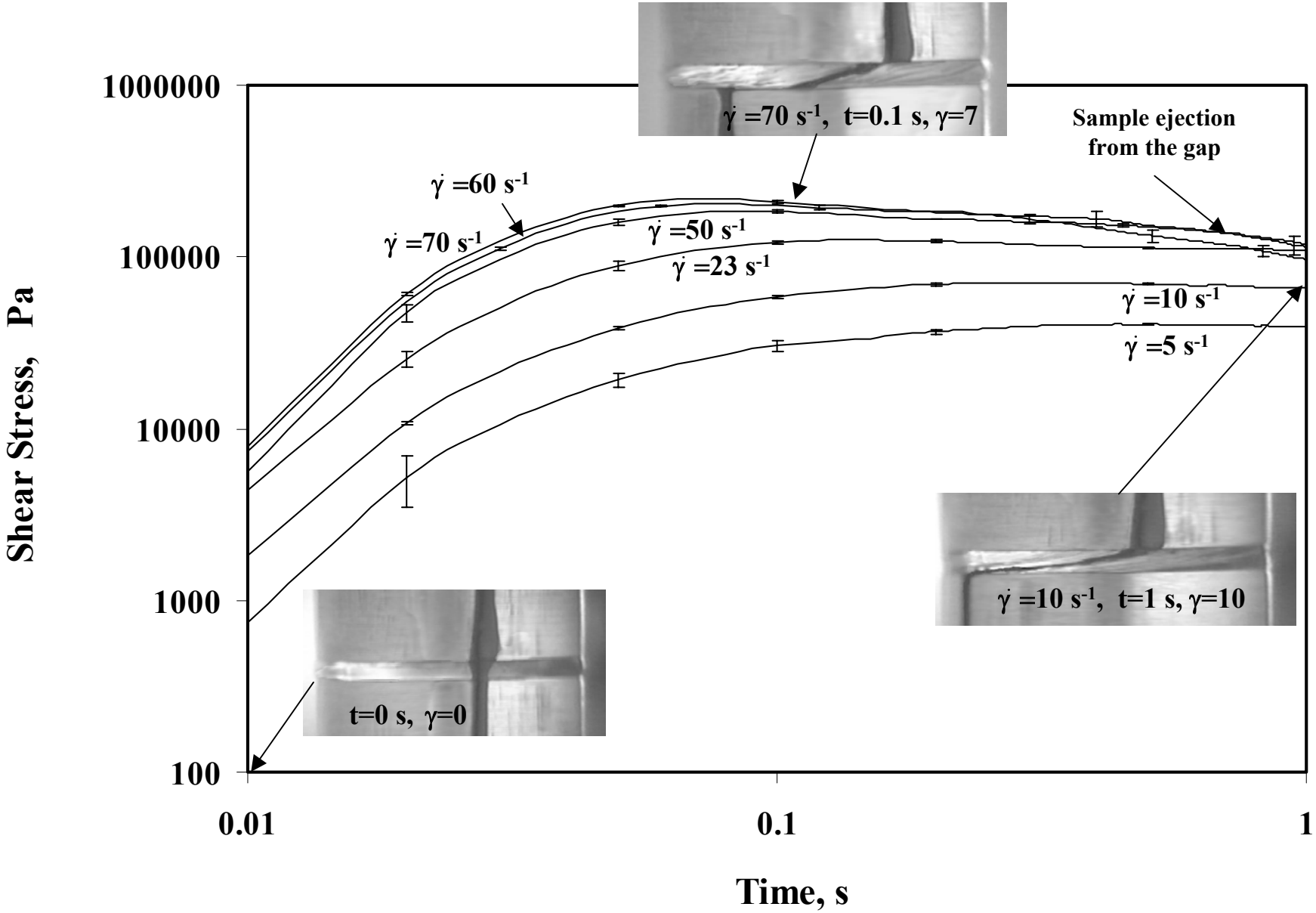

HDPE steady torsional flow

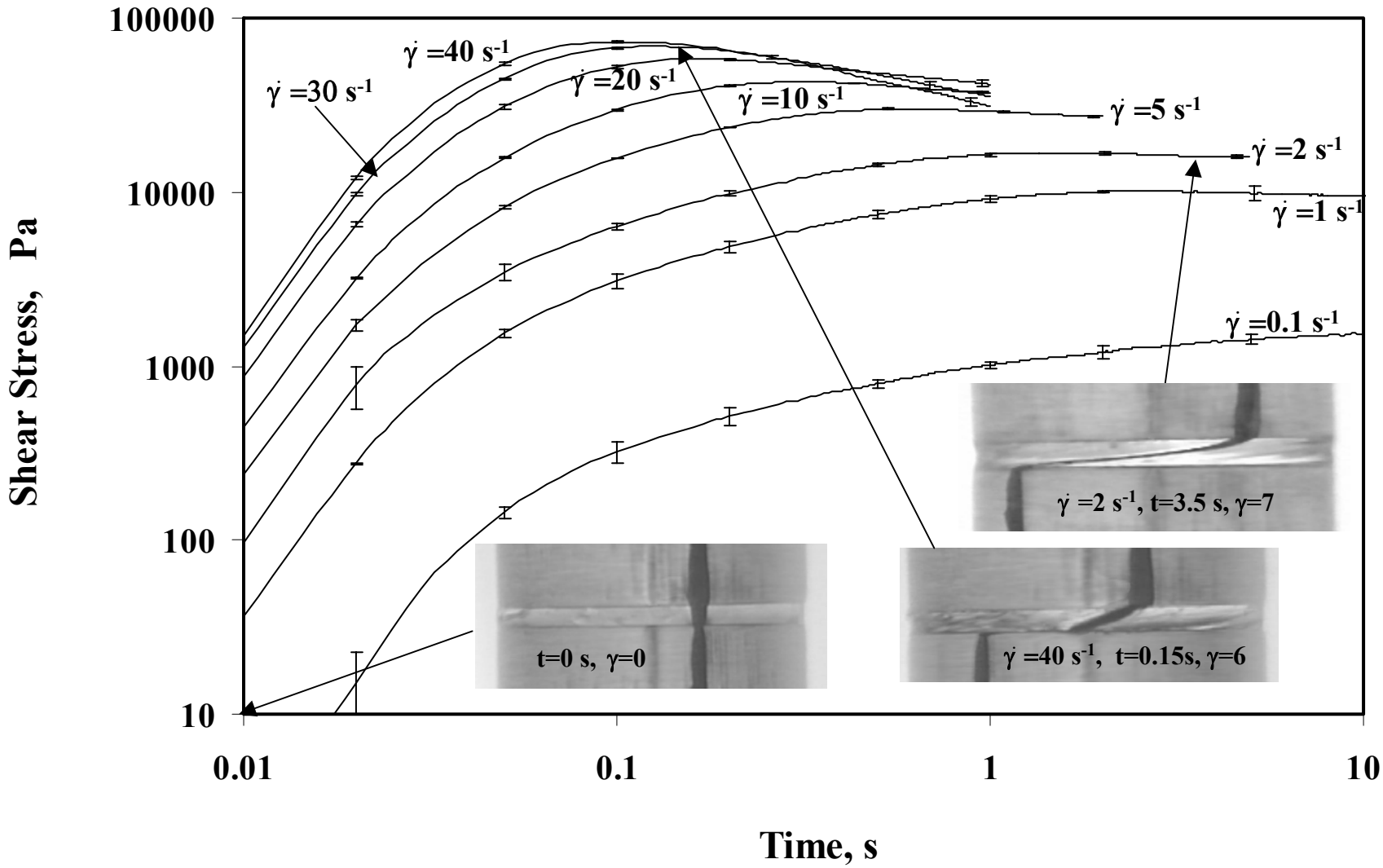

PDMS steady torsional flow

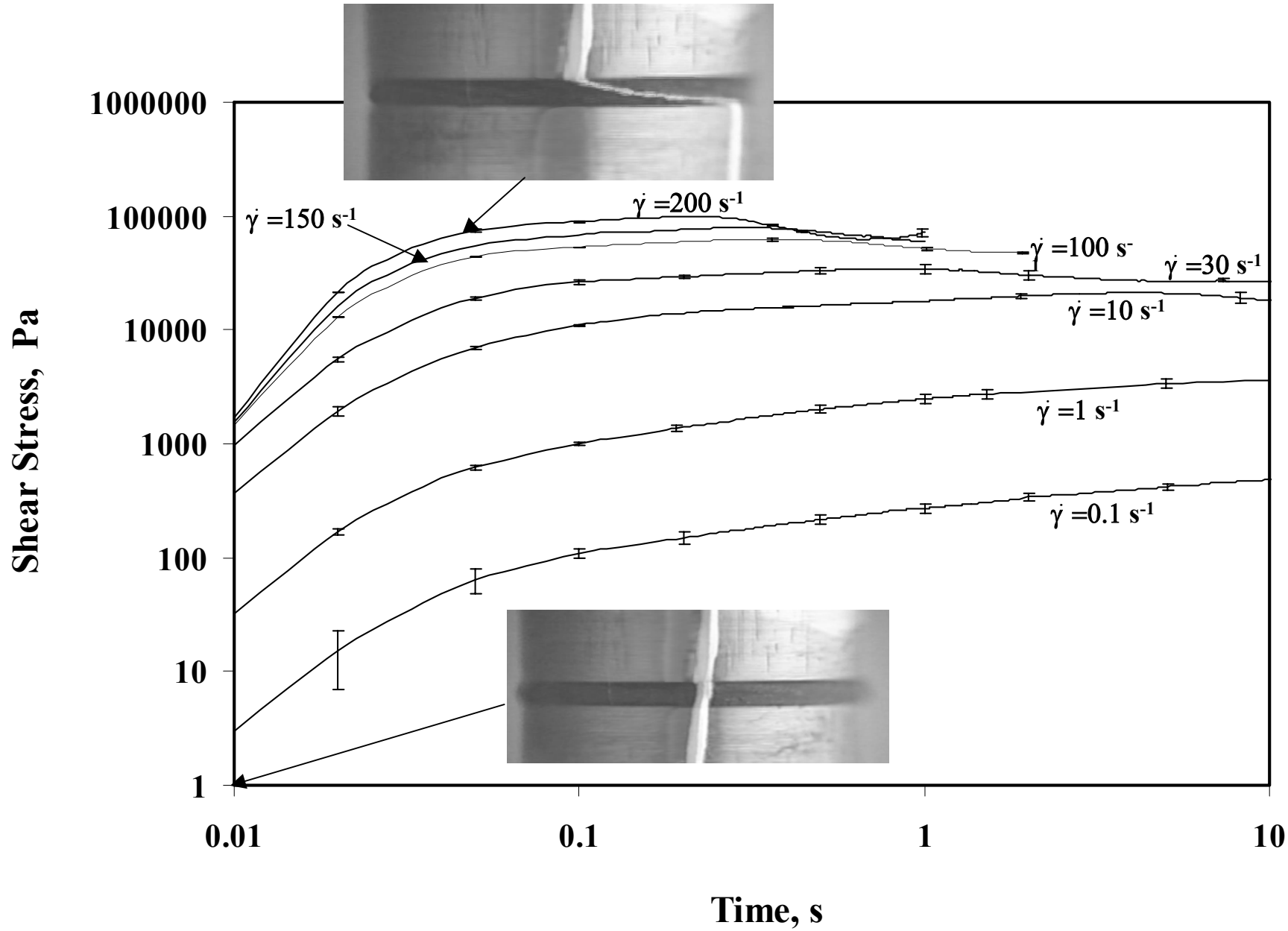

BAMO/AMMO TPE steady torsional flow

Critical wall shear stress values at which strong wall slip is initiated in steady torsional flow

- HDPE:
  - @ 170°C .22 MPa
  - @ 190°C .22 MPa
  - @ 210°C .23 MPa
- PDMS:
  - @ 10°C .067 MPa
  - @ 30°C .069 MPa
  - @ 50°C .068 Mpa
- No strong wall slip for BAMO/AMMO TPE for strains up to 20 even at shear rates as high as 200 s-1.

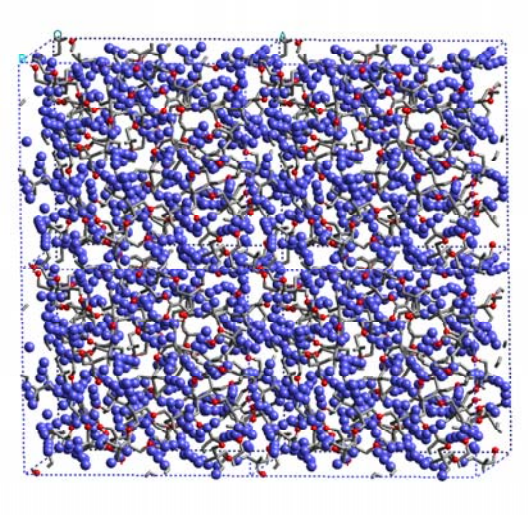

Bamo/Ammo (d=1.23 g/cm^3)

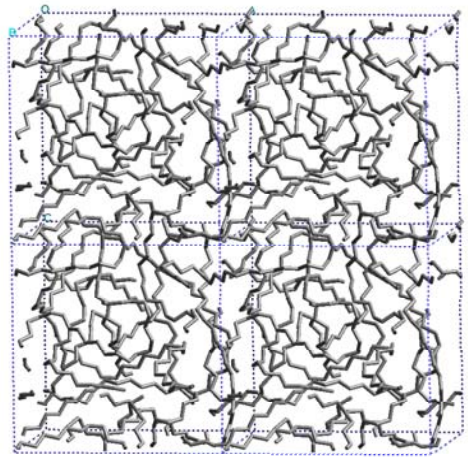

Polyethylene (d=0.88 g/cm^3)

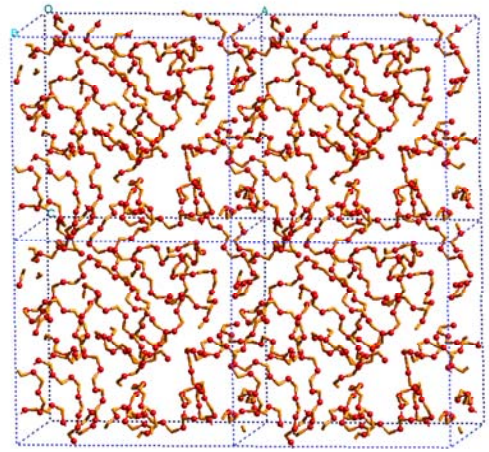

PDMS (d=1.28 g/cm^3)

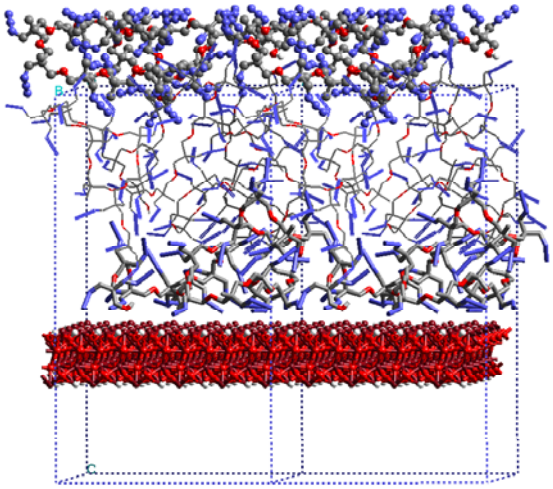

Bamo/Ammo (d=1.21 g/cm^3)-Fe_2O_3

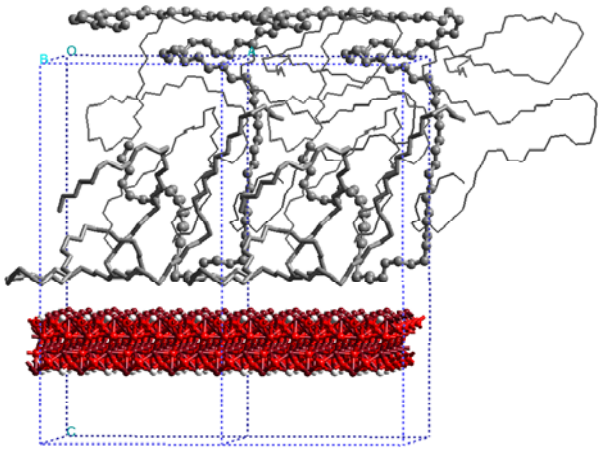

Pe (d=0.85 g/cm^3)-Fe_2O_3

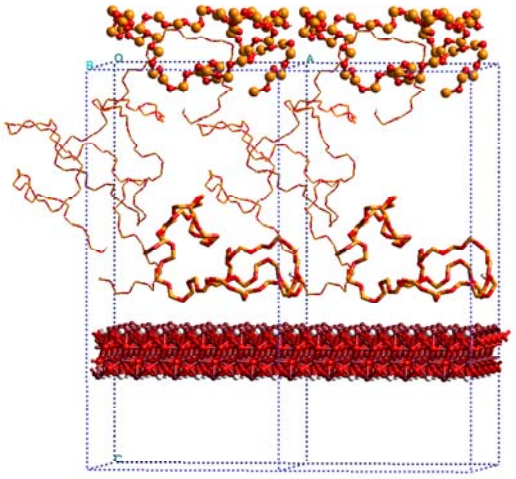

Pdms (d=1.08 g/cm^3) -Fe_2O_3

Simulated polymer melts and the polymer-metal interfaces are shown as 2axbx2c and 2axbxc respectively.

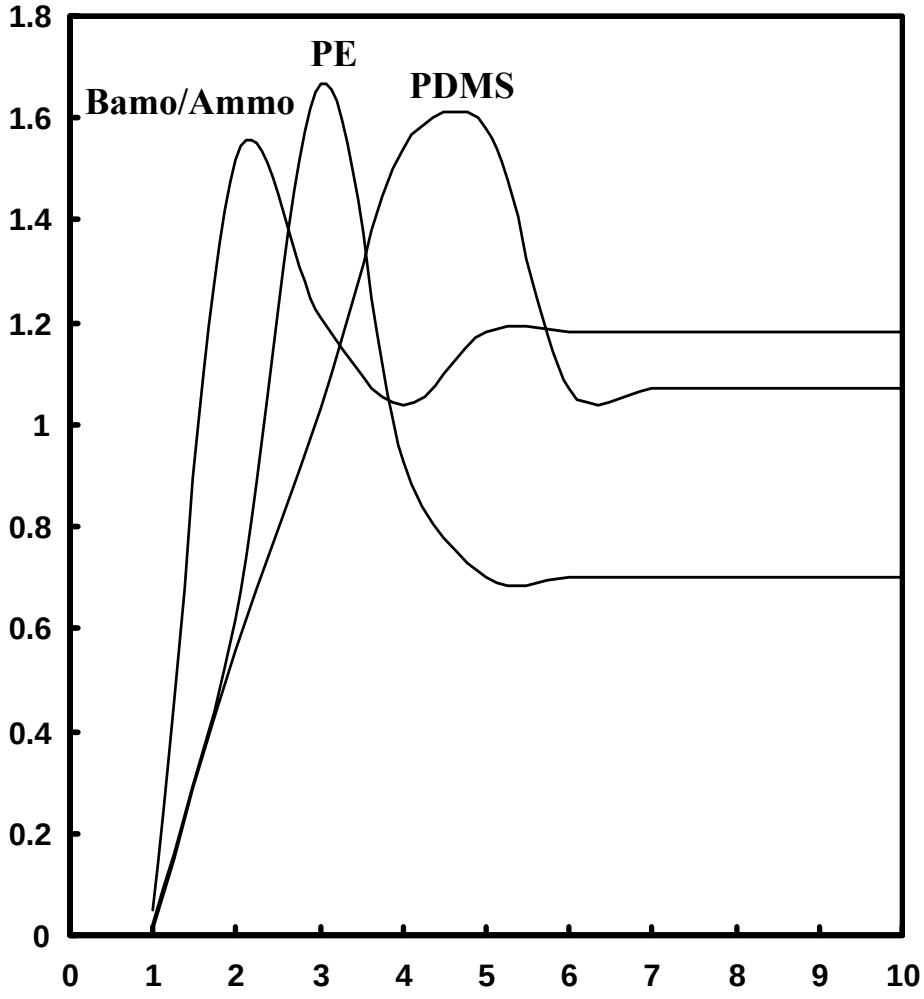

Polymer density versus distance from the metal surface.

Note: Both pdms and pe have showed similar structures of carbon and hydrogen atoms at the polymer-metal interface. Bamo/Ammo-metal interface is covered by large quantities of nitrogen atoms. Negatively charged nitrogen atoms (azido groups of Bamo/Ammo) are strongly interacting with the positively charged metal surface (H^+ and Fe^{+3}). Pdms and Pe have much more positively charged hydrogen atoms (CH2 for Pe and CH3 for Pdms) at the interface. Thus, they exhibit weaker adhesion properties to the metal compare to Bamo/Ammo. Nonbond interactions, Van Der Walls and Coulomb forces are higher for Bamo/ammo-metal interface due to the presence of opposite charges in short distances and higher density.

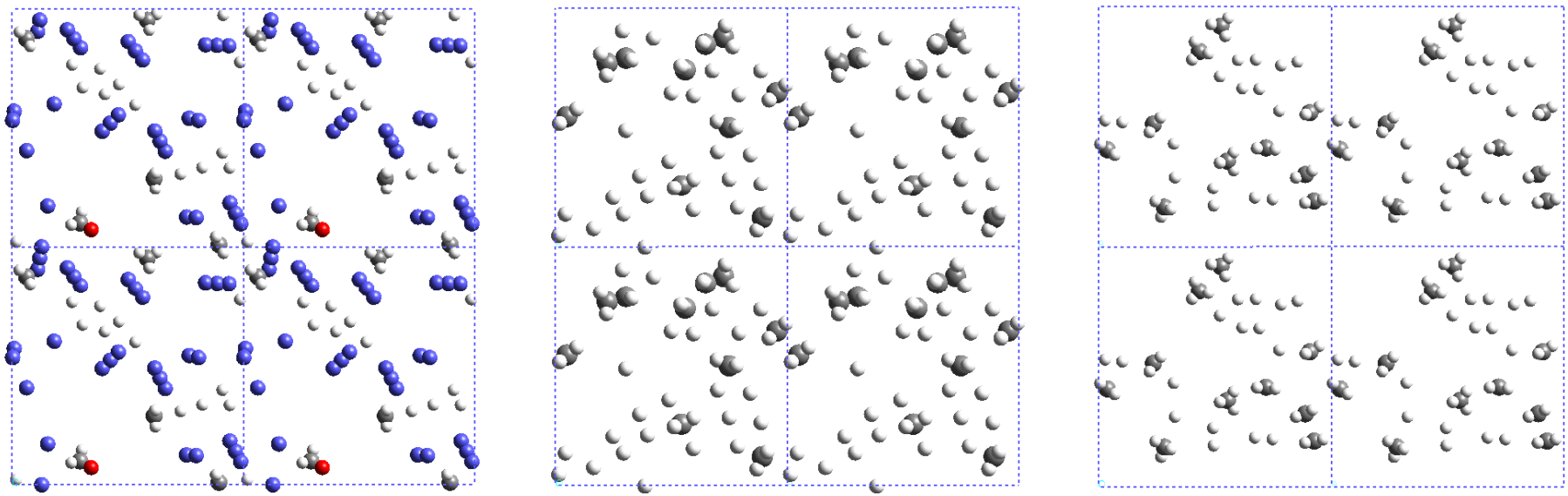

Bamo/Ammo

d=1.52 g/cm^3

Pe

d=0.62 g/cm^3

Pdms

d=0.56 g/cm^3

Figure 4. 1 Å depth slices of Bamo/Ammo, Pe and Pdms 2 Å above the metal wall, Fe_2O_3(111).

Table 1. Calculated cohesive energy values of BAMO/AMMO, HDPE and PDMS.

Polymer	Simulation Density (g/cm^3)	Coulomb Energy (cal/cm^3)	VDW Energy (cal/cm^3)	Hydrogen Bond Energy (cal/cm^3)	Cohesive Energy (cal/cm^3)
BAMMO/AMMO	1.23	42.83	38.19	0.39	81.4
HDPE	0.88	67.64	1.74	0	69
PDMS	1.28	58.58	2.97	0	61.5

Table 3. Calculated solubility parameters of BAMO/AMMO, HDPE and PDMS.

Polymer	Simulation Density (g/cm^3)	Cohesive Energy (E_{CED}) (cal/cm^3)	Solubility Parameter $\delta = (E_{CED})^{1/2}$	Solubility Parameter $\delta = \rho . \sum G/M$
BAMO/AMMO	1.23	81.4	9.02	9.58
HDPE	0.88	69	8.33	8.36
PDMS	1.28	61.5	7.84	8.17

Table 2. Calculated adhesive energy values of BAMO/AMMO, HDPE and PDMS melts with the iron wall.

Polymer-Iron Interface	Simulation Density (g/cm^3)	Coulomb Energy (cal/cm^3)	VDW Energy (cal/cm^3)	Hydrogen Bond Energy (cal/cm^3)	Adhesive Energy (cal/cm^3)
BAMO/AMMO-Fe	1.21	1642	87	12	1741
HDPE-Fe	0.85	545	151	0	974
PDMS-Fe	1.08	853	121	0	696

Conclusions

- The shear stress at the onset of catastrophic failure of the no-slip condition in steady torsional flow coincides with onset of flow instabilities in capillary flow
- TPE which does not exhibit strong slip up to high strains (20) and strain rates (200s-1) in steady torsional flow also does not exhibit flow instabilities in capillary flow

Conclusions

- The critical shear stress at the point of catastrophic failure of the no-slip condition is temperature independent for PDMS and HDPE.
- Results emphasize the central role played by wall slip in the development of the flow instabilities

What happens to development of surface irregularities in extrusion flow when we fill these polymers with rigid fillers?

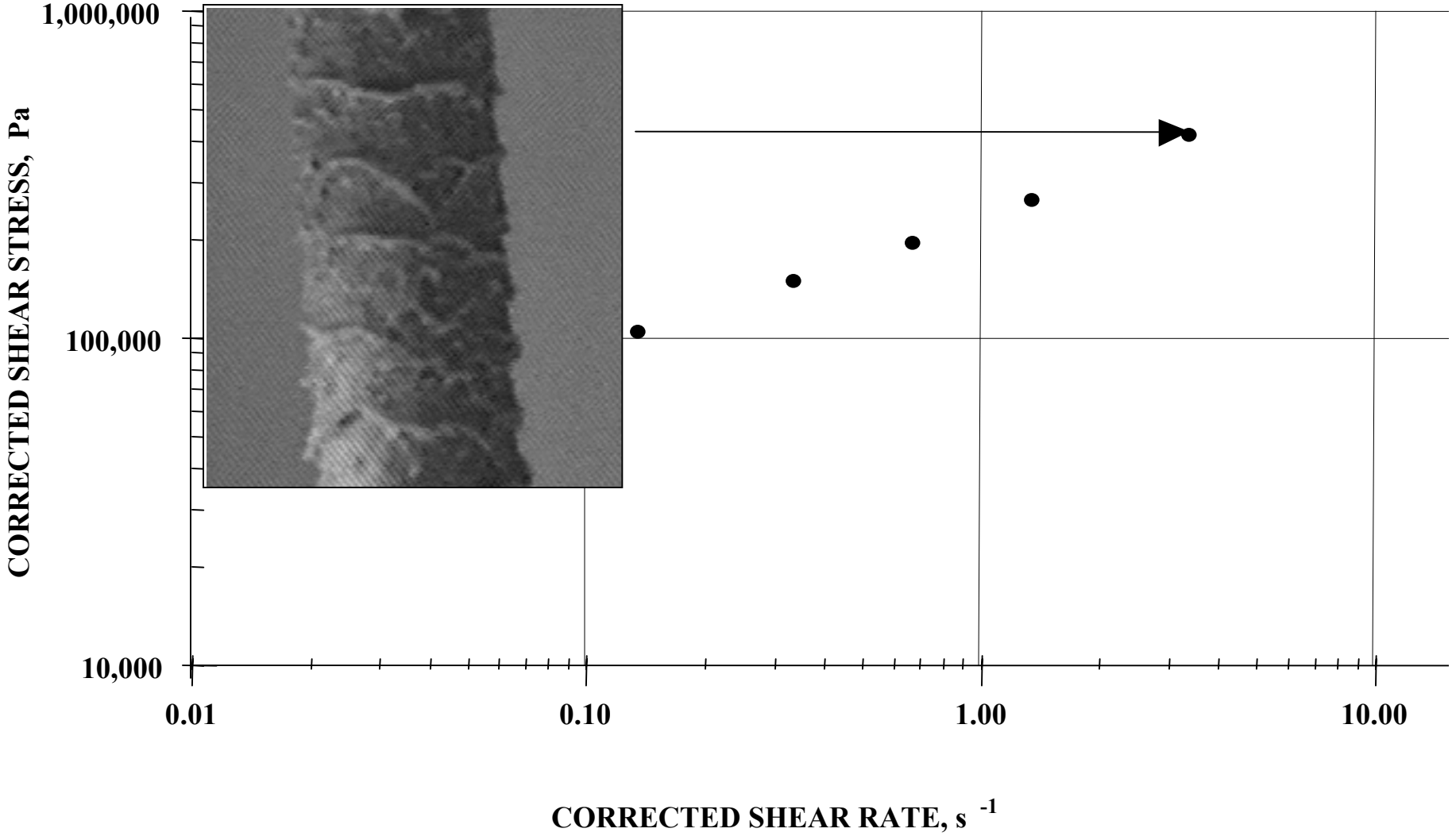

KCl filled BAMO/AMMO TPE

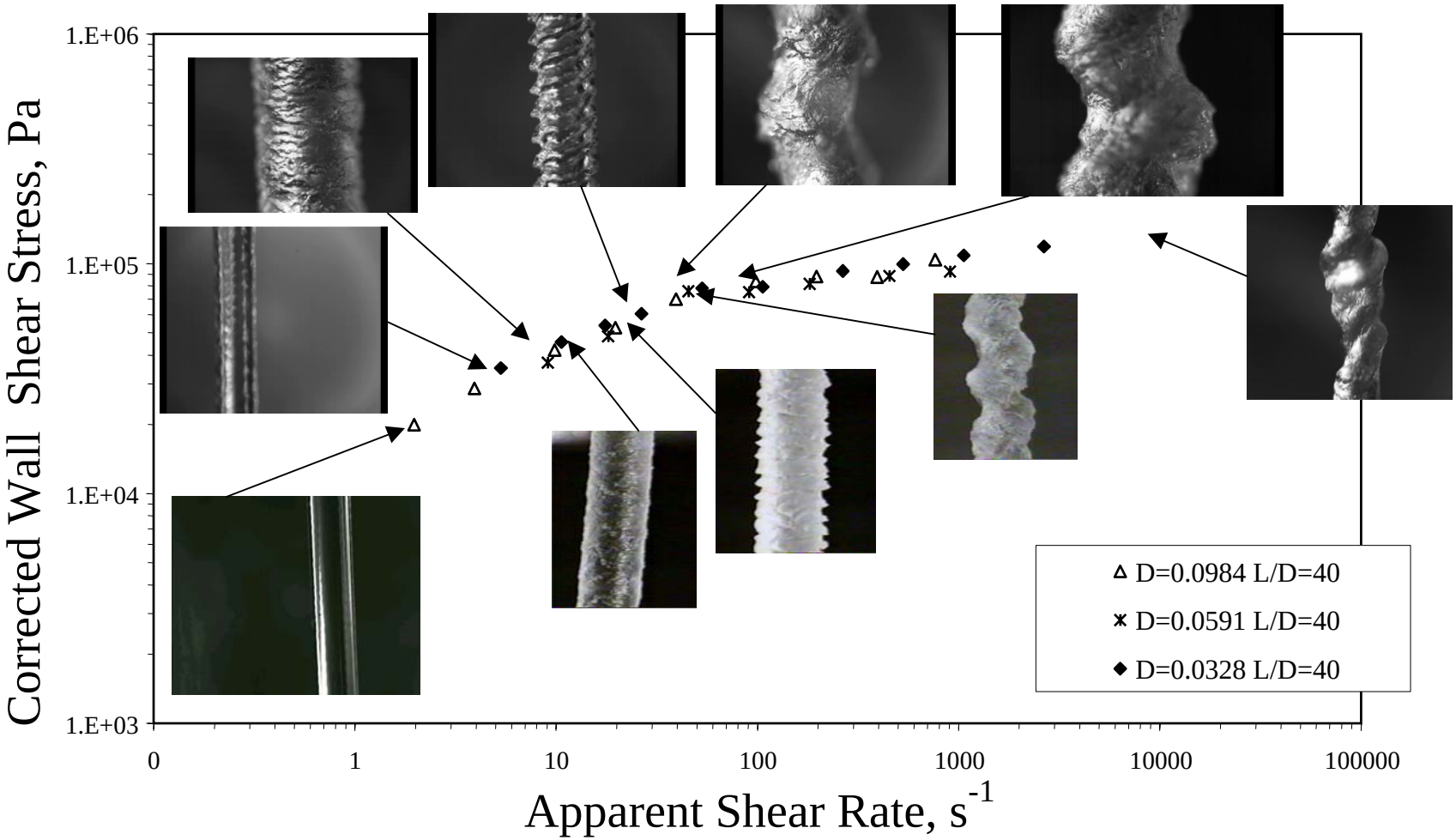

Flow curves and extrudates of poly(dimethyl siloxane) collected with capillaries with different diameters and development of extrudate surface irregularities

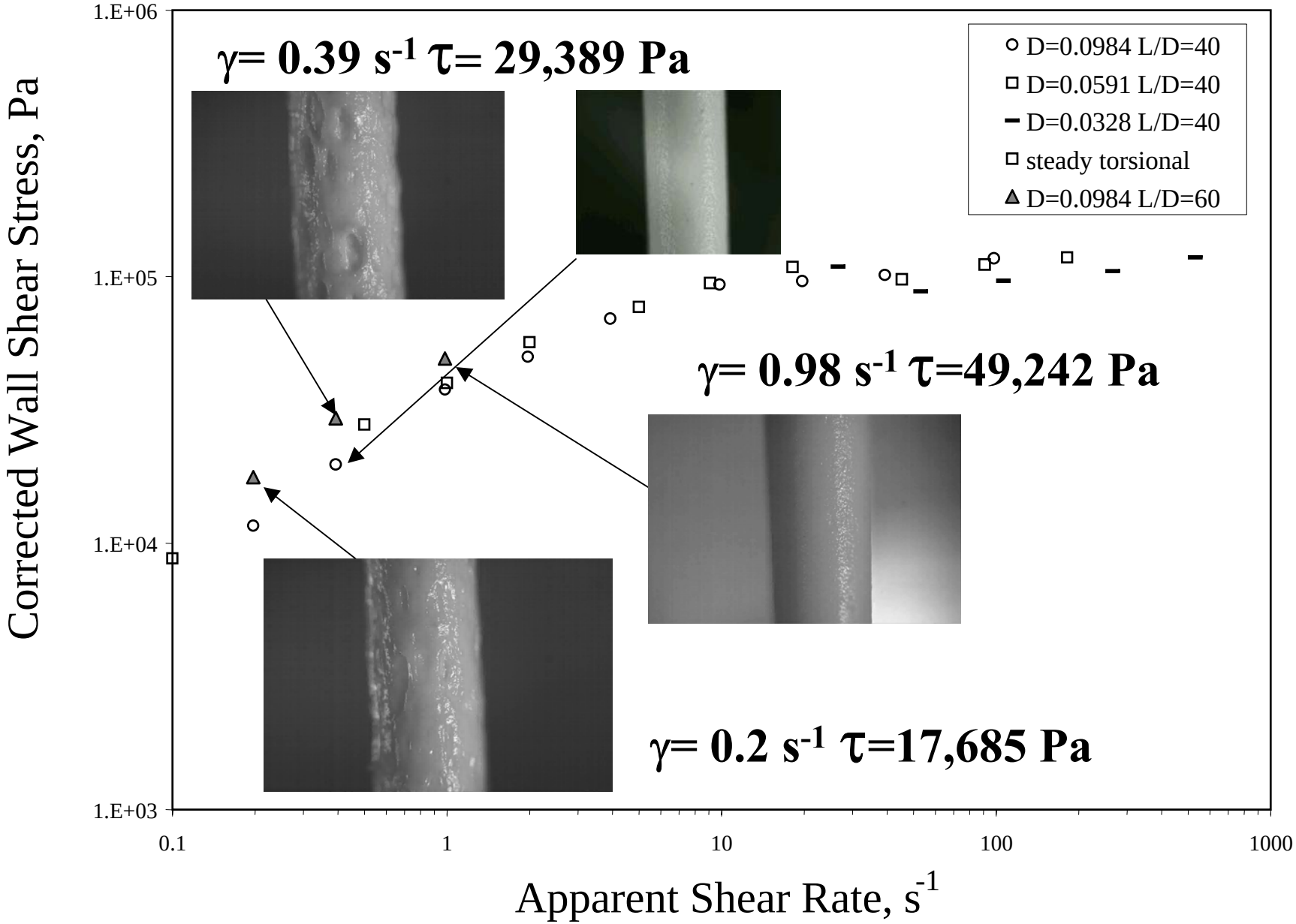

Flow curves and extrudates of suspension of poly(dimethyl siloxane) PDMS incorporated with 40% by volume of glass spheres collected with capillaries with different diameters.

Frame work for the analysis to follow:

- Ab Initio and molecular dynamics calculations to differentiate the wall interactions of various polymers and various metal surfaces
- Steady state solution of Equations of Motion with wall slip velocity (normal and shear stress dependent) and compressible melt/suspension
- Time dependent solution of Equations of Motion with wall slip condition (normal and shear stress dependent) and compressible melt/suspension

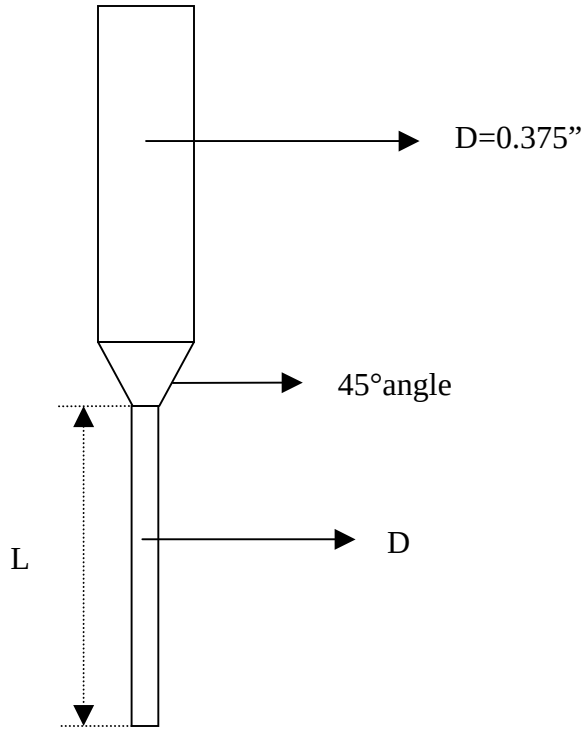

The angle of convergence was varied between 15, 45 and 75 degrees.

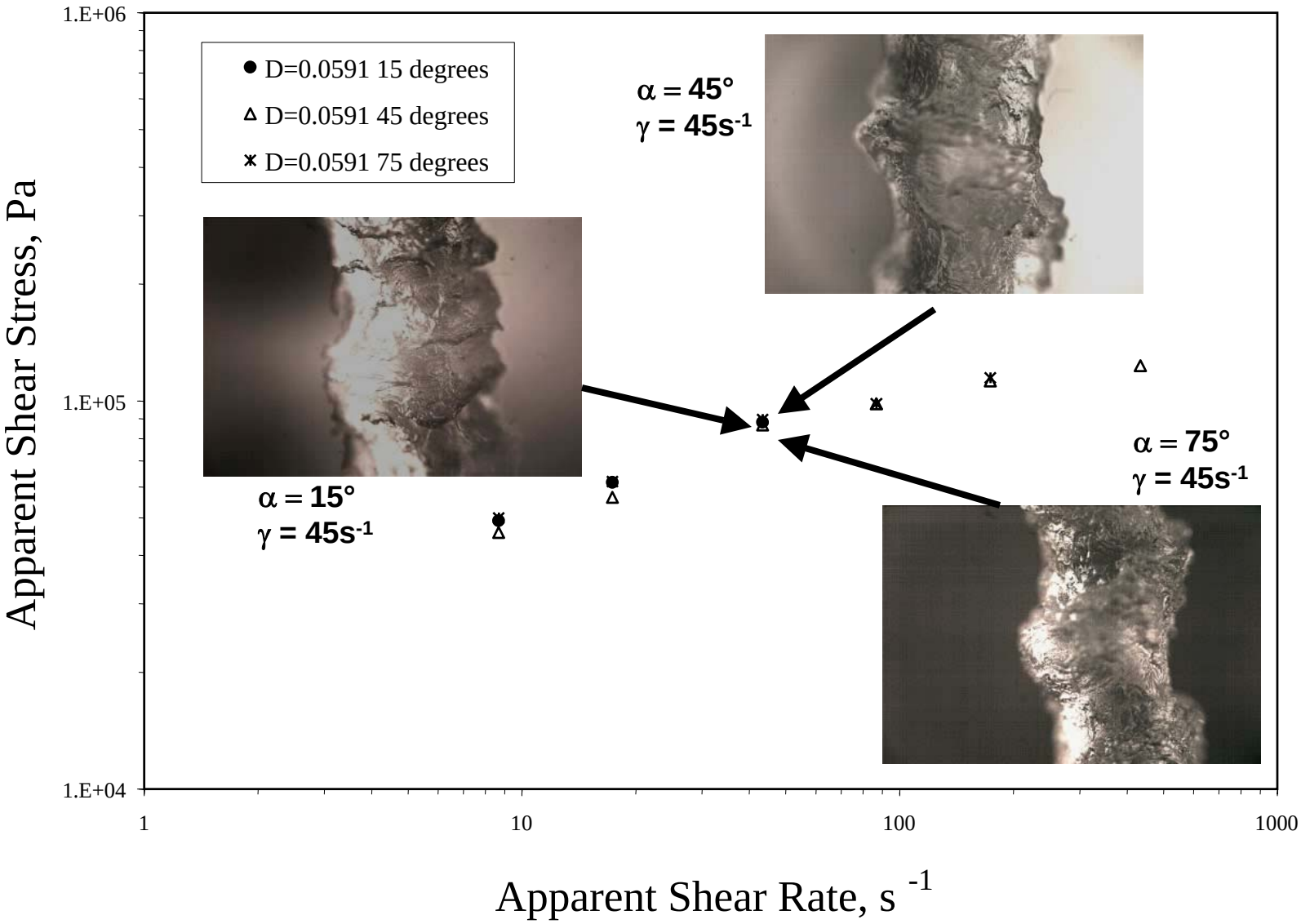

Pure PDMS

Apparent Shear Stress vs. Apparent Shear Rate Behavior: Comparison of Different Converging Entry Angles

Mathematically model only flow through a circular tube (Poiseuille flow) subject to wall slip

Compressibility of the polymer melt and polymeric suspensions

Evidence for the importance of compressibility

The elastomer is opaque when significant air is introduced in the extruder

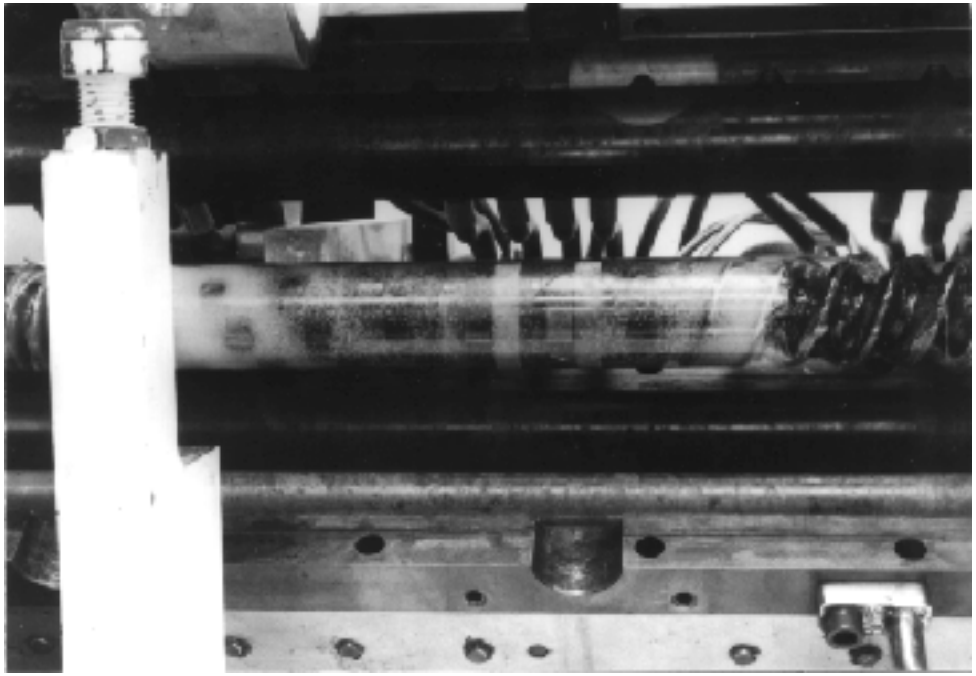

Entrainment of Air into Filled Polymers: Demo using x-ray Radiography

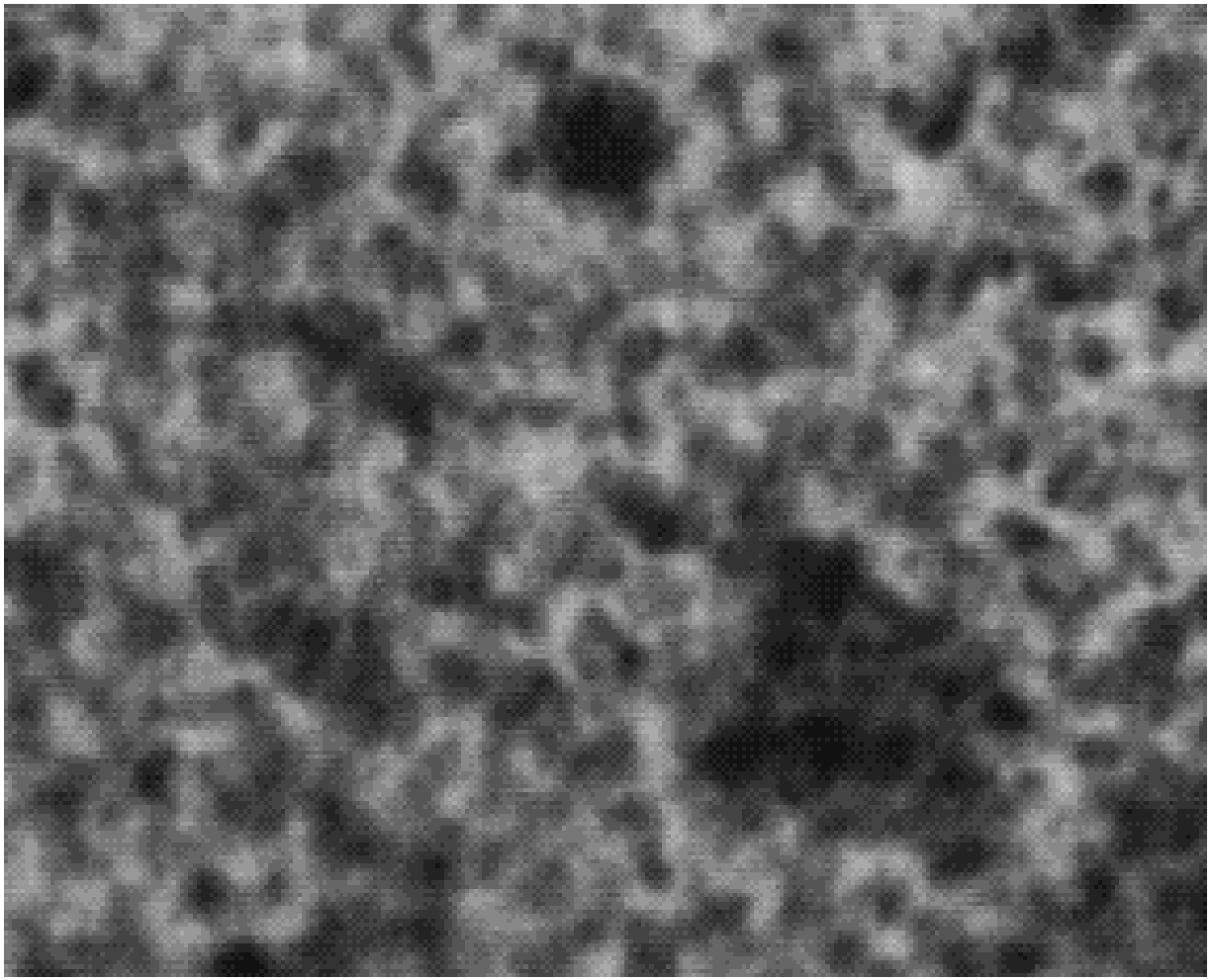

Air Entrainment into Filled Polymers: Demo using MRI

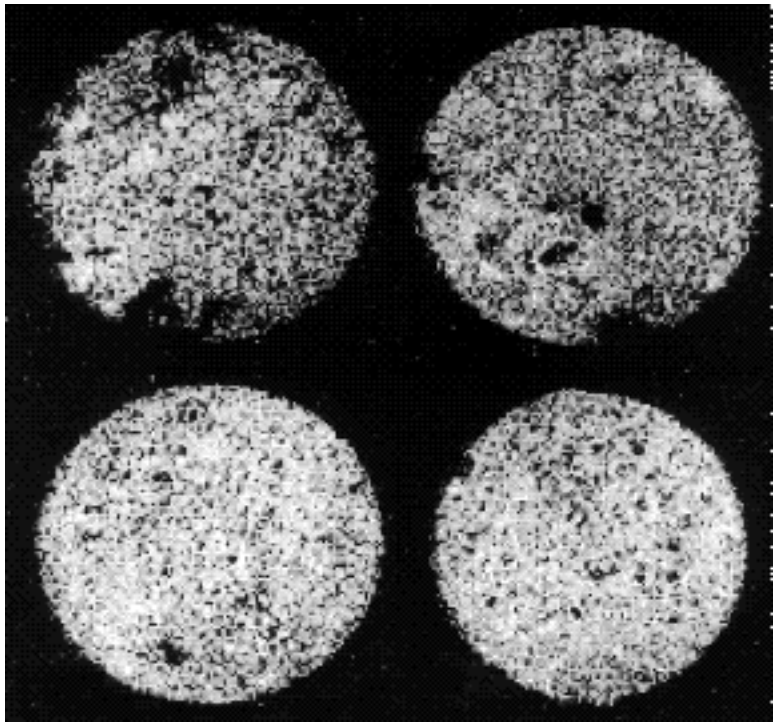

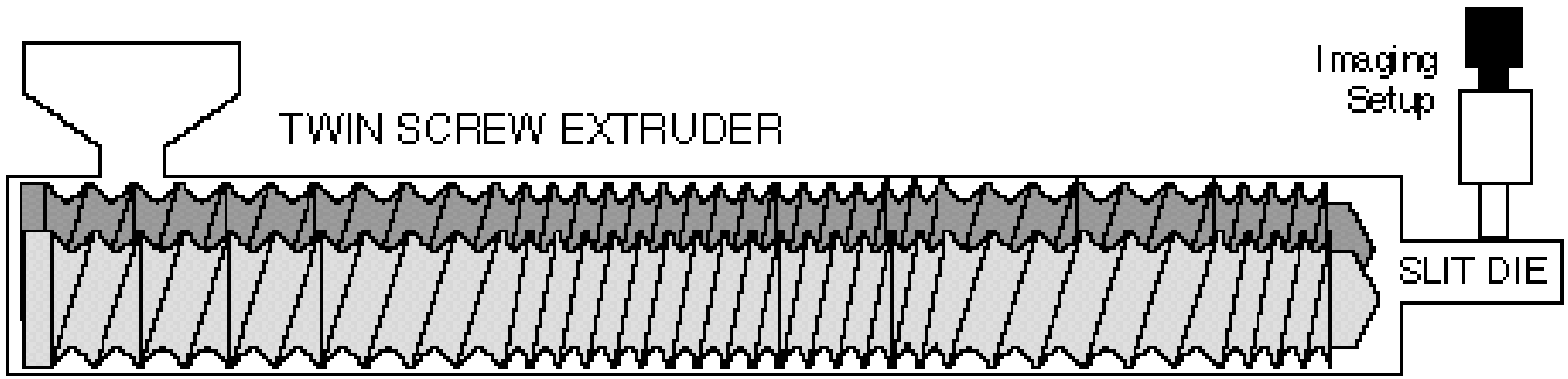

Figure 1

Air lubricates the wall of the die at exit of the die

Camera at 500-1000 fps

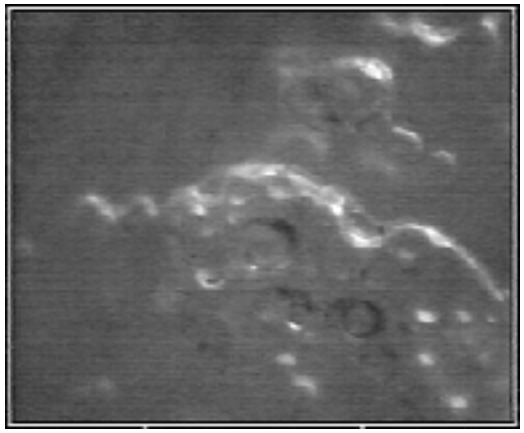

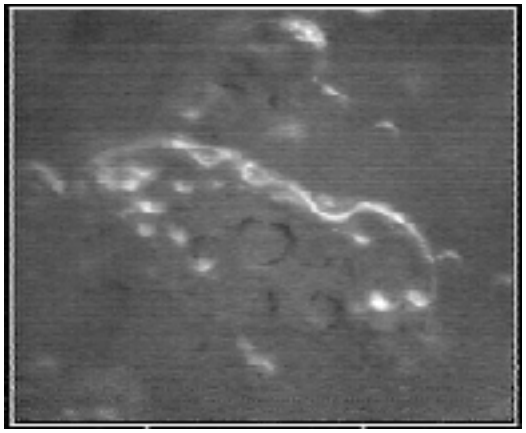

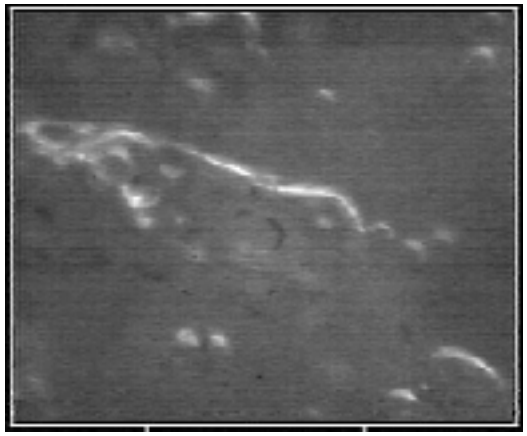

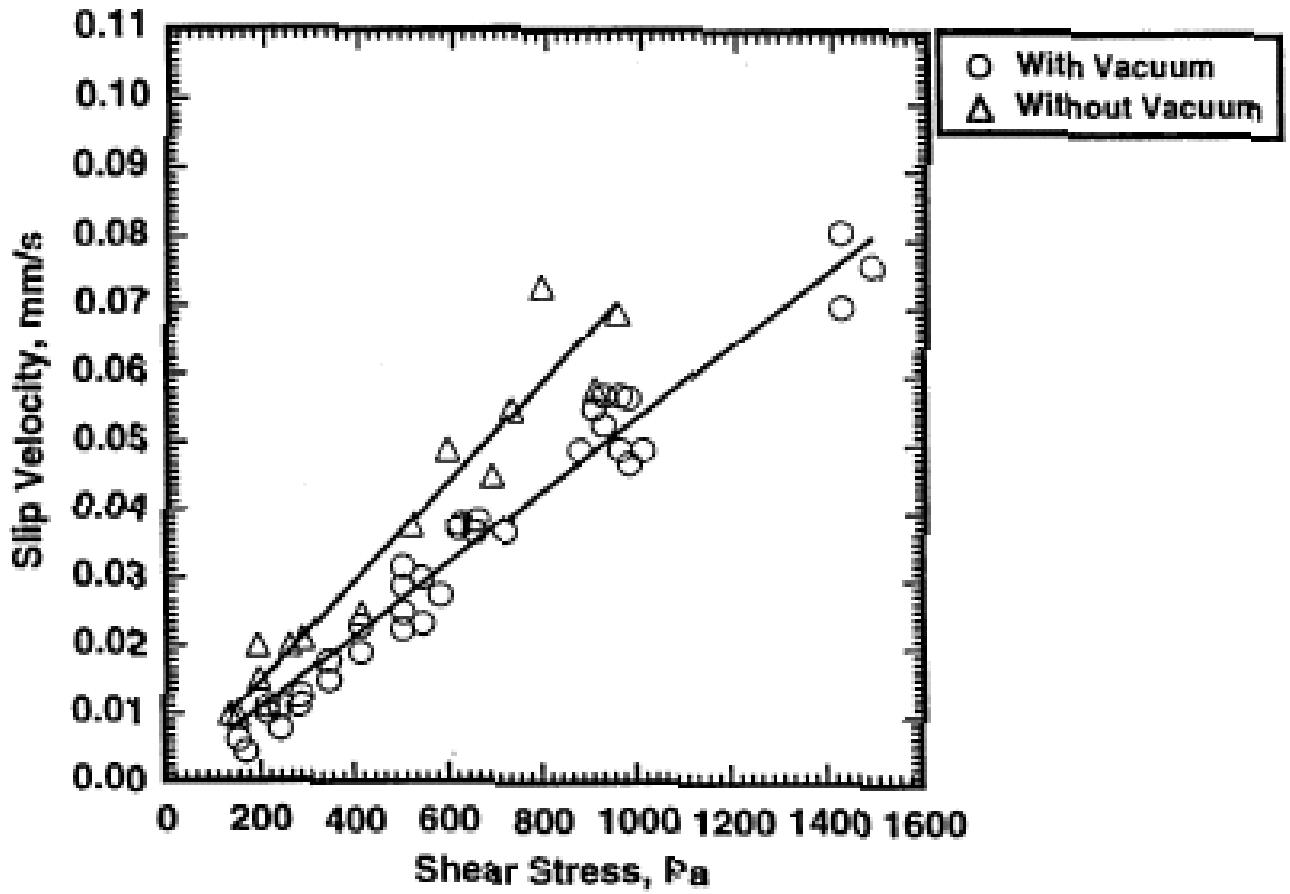

Fig. 6 Slip velocity versus shear stress behavior of suspension samples processed with and without vacuum/devolatilization.

Density, ρ varies with pressure P: constants γ and γ_1

$$\rho = \gamma p + \gamma_1$$

Slip velocity, Us, versus shear stress, τ_w:
Parameters are β, sb, α.

$$u_s = \beta \tau_w^{sb} \left(1 + \tanh\left(\alpha(\tau_w - \tau_a)\right)\right)$$

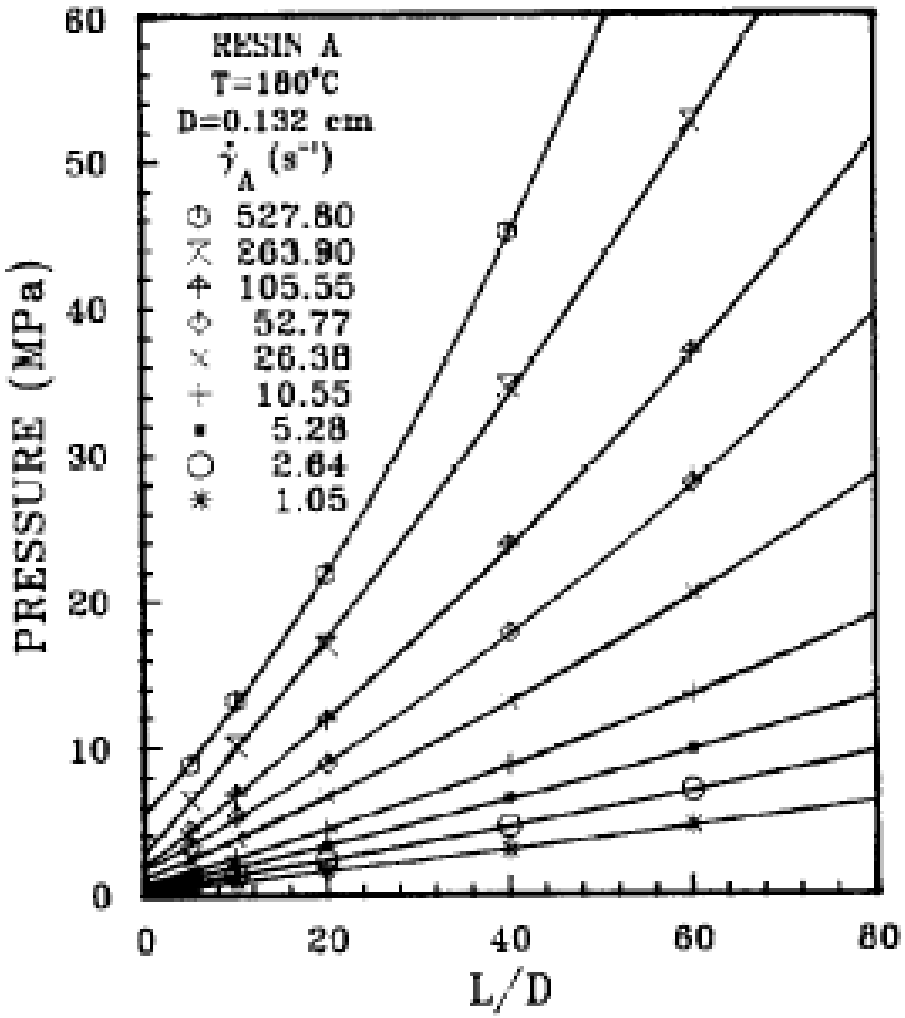

Change in pressure gradient with increasing pressure is indicative of effect of pressure on wall slip behavior.
<u>Slip decreases with Increasing pressure.</u>

Data: High density polyethylene at 180 °C
(Hatzikiriakos and Dealy, J. Rheology, 36, 703 (1992).

$$\beta = \beta_0 (p_a / p)^{\kappa}$$

$$\frac{\partial p}{\partial t} + \frac{\partial}{\partial z}\left[\left(p + \frac{\gamma_1}{\gamma}\right)V\right] = 0$$

$$\frac{\partial V}{\partial t} + \frac{2\tau_w}{(\gamma p + \gamma_1)R} + \frac{1}{\gamma p + \gamma_1}\frac{\partial p}{\partial z} = 0$$

V is the mean velocity in the channel in z-direction, t is time, P is pressure, τ_w is the wall shear stress.

Under lubrication flow assumptions

$$\tau_w = -\frac{R}{2}\left(\frac{dp}{dz}\right) + \frac{35R}{18}\frac{d\tau_w}{dz}$$

where τ_w is the wall shear stress, R is the radius, P is pressure

[Hatzikiriakos and Dealy, J. Rheology, 36, 703 (1992)].

Under lubrication flow assumptions

$$\tau_w = -\frac{R}{2}\left(\frac{dp}{dz}\right) + \frac{35R}{18}\frac{d\tau_w}{dz}$$

Determined to be small

Therefore the shear stress at the wall, τ_w is linked only to local pressure gradient.

Use generalized Newtonian fluid constitutive equation:

$$\underline{\tau} = \eta(II) * \underline{\Delta}$$

where $\underline{\tau}$ and $\underline{\Delta}$
are stress and rate of
deformation tensors;
$\eta(II)$ is the shear viscosity material function

Viscoplastic Hershel Bulkley equation to describe the shear viscosity.

$$\begin{cases} \tau_{rz} = -m\left|\dfrac{\partial u_z}{\partial r}\right|^{n-1}\dfrac{\partial u_z}{\partial r} \pm \tau_y, & |\tau_{rz}| > \tau_y, \\ \dfrac{\partial u_z}{\partial r} = 0, & |\tau_{rz}| \le \tau_y. \end{cases}$$

τ_y is the yield stress, m is the consistency index and n is the power law index. This reduces to a power law fluid model when τ_y is zero.

Under steady state conditions there is an analytical solution for local mean velocity V:

$$
V = \begin{cases}
-\dfrac{16\tau_y}{R^2 m^{1/n}(1+1/n)(3+1/n)}\left[-\tau_y - \dfrac{R}{2}\left(\dfrac{\partial p}{\partial z}\right)_s\right]^{2+1/n}\left(-\dfrac{\partial p}{\partial z}\right)_s^{-3} \\
\quad -\dfrac{16}{R^2 m^{1/n}(1+1/n)(2+1/n)}\left[-\tau_y - \dfrac{R}{2}\left(\dfrac{\partial p}{\partial z}\right)_s\right]^{3+1/n}\left(-\dfrac{\partial p}{\partial z}\right)_s^{-3} \\
\quad +\dfrac{16\tau_y}{m^{1/n}(1+1/n)}\left[-\tau_y - \dfrac{R}{2}\left(\dfrac{\partial p}{\partial z}\right)_s\right]^{1+1/n}\left(-\dfrac{\partial p}{\partial z}\right)_s^{-1} \\
\quad +\beta\left[-\dfrac{R}{2}\left(\dfrac{\partial p}{\partial z}\right)_s\right]^{sb}\left[1+1\tanh\left(\alpha\left(-\dfrac{R}{2}\left(\dfrac{\partial p}{\partial z}\right)_s - \tau_a\right)\right)\right], & \dfrac{R}{2}\left(\dfrac{\partial p}{\partial z}\right)_s > \tau_y, \\
\\
\beta\left[-\dfrac{R}{2}\left(\dfrac{dp}{dz}\right)_s\right]^{sb}\left[1+1\tanh\left(\alpha\left(-\dfrac{R}{2}\left(\dfrac{\partial p}{\partial z}\right)_s - \tau_a\right)\right)\right], & \dfrac{R}{2}\left(\dfrac{\partial p}{\partial z}\right)_s \le \tau_y.
\end{cases}
$$

Solve numerically using finite differences (Predictor-Corrector):

$$\frac{\hat{p}_{i+1/2} - p^l_{i+1/2}}{\Delta t} + \frac{\left((p^l_{i+3/2} + p^l_{i+1/2})/2 + \gamma_1/\gamma\right)V^l_{i+1} - \left((p^l_{i+1/2} + p^l_{i-1/2})/2 + \gamma_1/\gamma\right)V^l_i}{\Delta z} = 0$$

$$\frac{\hat{V}_i - V^l_i}{\Delta t} + \frac{2\tau_{wi}^{\ l}}{\left(\gamma(p^l_{i-1/2} + p^l_{i+1/2})/2 + \gamma_1\right)R} + \frac{1}{\left(\gamma(p^l_{i-1/2} + p^l_{i+1/2})/2 + \gamma_1\right)}\frac{p^l_{i+1/2} - p^l_{i-1/2}}{\Delta z} = 0$$

$$\tau_{wi}^{\ l} = -\frac{R}{2}\left(\frac{\partial p}{\partial z}\right)_{si}^{l} \qquad V_i^l = F\left[\left(\frac{\partial p}{\partial z}\right)_{si}^{l}\right]$$

Δt time step, Δz grid spacing, l is the time step index, and
F is the function to obtain steady state value of mean velocity V

$$\frac{p_{i+1/2}^{l+1} - p_{i+1/2}^{l}}{\Delta t} + \frac{\left((p_{i+3/2}^{l} + p_{i+1/2}^{l})/2 + \gamma_1/\gamma\right)V_{i+1}^{l} - \left((p_{i+1/2}^{l} + p_{i-1/2}^{l})/2 + \gamma_1/\gamma\right)V_{i}^{l}}{2\Delta z}$$

$$+ \frac{\left(\hat{p}_{i+3/2} + \hat{p}_{i+1/2})/2 + \gamma_1/\gamma\right)\hat{V}_{i+1} - \left((\hat{p}_{i+1/2} + \hat{p}_{i-1/2})/2 + \gamma_1/\gamma\right)\hat{V}_{i}}{2\Delta z} = 0$$

$$\frac{V_i^{l+1} - V_i^{l}}{\Delta t} + \frac{2\tau_{wi}^{\ l}}{\left(\hat{p}_{i+3/2} + \hat{p}_{i+1/2})/2 + \gamma_1/\gamma\right)R} + \frac{2\hat{\tau}_{wi}}{\left(\hat{p}_{i+3/2} + \hat{p}_{i+1/2})/2 + \gamma_1/\gamma\right)R}$$

$$+ \frac{1}{\left(\gamma(p_{i-1/2}^{l} + p_{i+1/2}^{l})/2 + \gamma_1\right)}\frac{p_{i+1/2}^{l} - p_{i-1/2}^{l}}{\Delta z} + \frac{1}{\left(\gamma(\hat{p}_{i-1/2} + \hat{p}_{i+1/2})/2 + \gamma_1\right)}\frac{\hat{p}_{i+1/2} - \hat{p}_{i-1/2}}{\Delta z} = 0$$

$$\hat{\tau}_{wi} = -\frac{R}{2}\left(\frac{\partial \hat{p}}{\partial z}\right)_{si} \qquad \hat{V}_i = F\left[\left(\frac{\partial \hat{p}}{\partial z}\right)_{si}\right]$$

Corrector step.

$$V = V_0, \qquad z = 0$$

$$p = p_a, \qquad z = L$$

Filled PDMS (40%)

Poly(dimethyl siloxane) with 40% solids:

$$u_s = \beta \tau_w^{sb} \left(1 + \tanh\left(\alpha(\tau_w - \tau_a)\right)\right)$$

$$\beta = \beta_0 (p_a / p)^{\kappa}$$

Critical wall shear stress at which
strong wall slip is observed:
$\tau_a =$ **35,000 Pa**

$m = 47600\, Pa \cdot s^{0.15}$, $n = 0.15$, $\gamma = 1.6 \times 10^{-6}\, m \cdot s^{-2}$, $\gamma_1 = 1073.4\, kg \cdot m^{-3}$

$\tau_y = 40000\, Pa$, $\beta_0 = 3.5 \times 10^{-13}\, \mathrm{m \cdot s^{-1} \cdot Pa^{-2.17}}$,

$\kappa = 0.3$, and $sb = 2.17$.

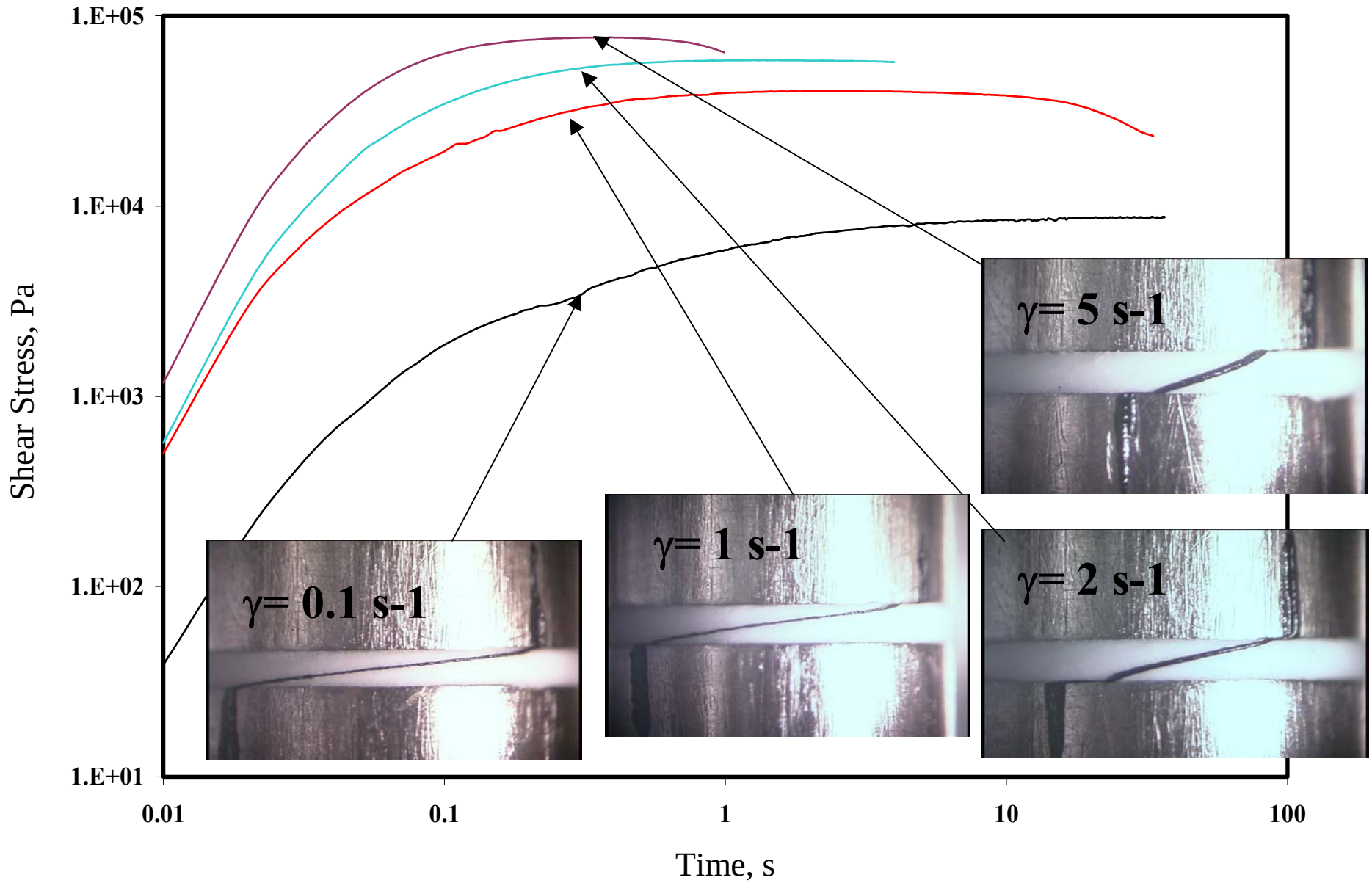

Steady torsional flow of poly (dimethyl siloxane) with 40% glass spheres at various apparent shear rates and results of straight-line marker technique applied at the free surface of 40% filled PDMS

PDMS with 40% glass spheres:
Slip velocity, Us vs wall shear stress τ_w :

$$u_s = \beta \tau_w^{sb} \left(1 + \tanh\left(\alpha(\tau_w - \tau_a)\right)\right)$$

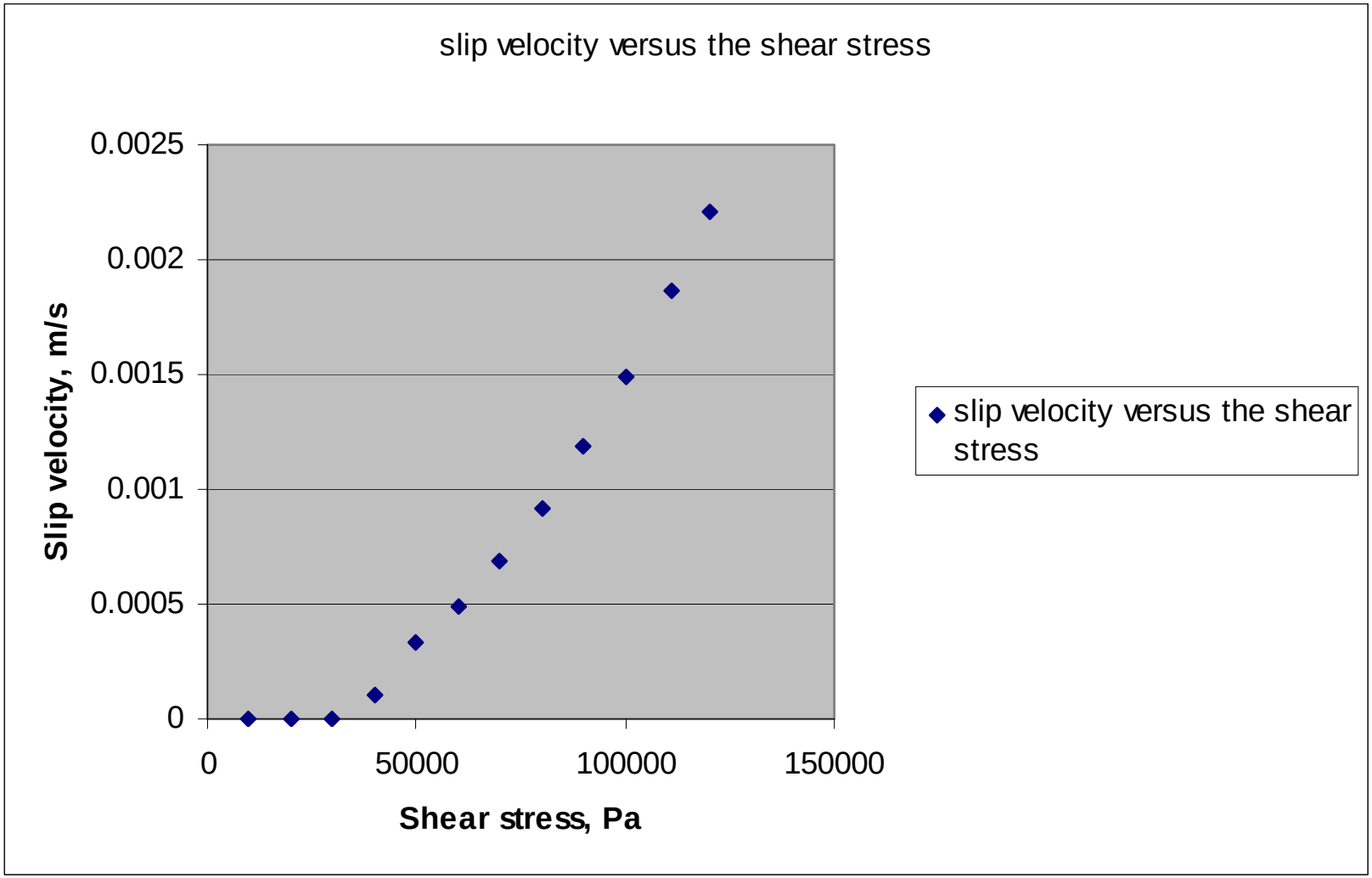

PDMS 40% glass

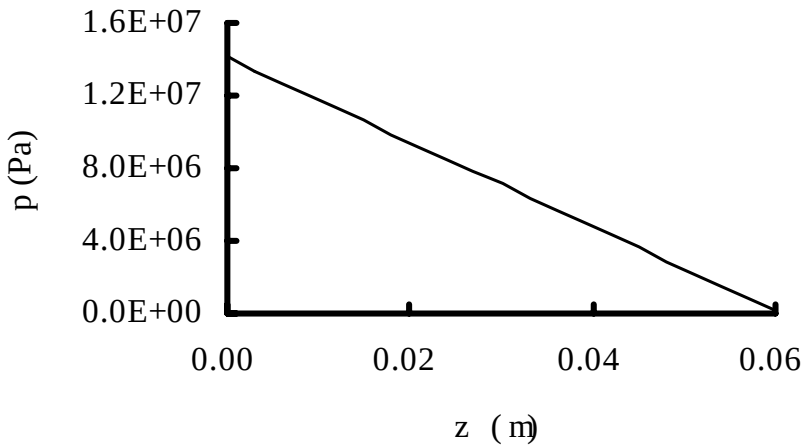

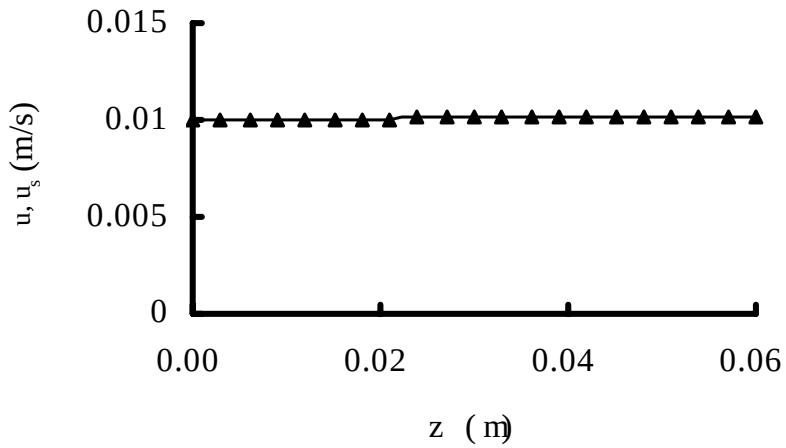

Solution for flow of PDMS suspension with 40% by volume glass
2R=0.0015m, L/2R=40, V_0=0.01m/s.
In the figure, triangles represent slip velocity.

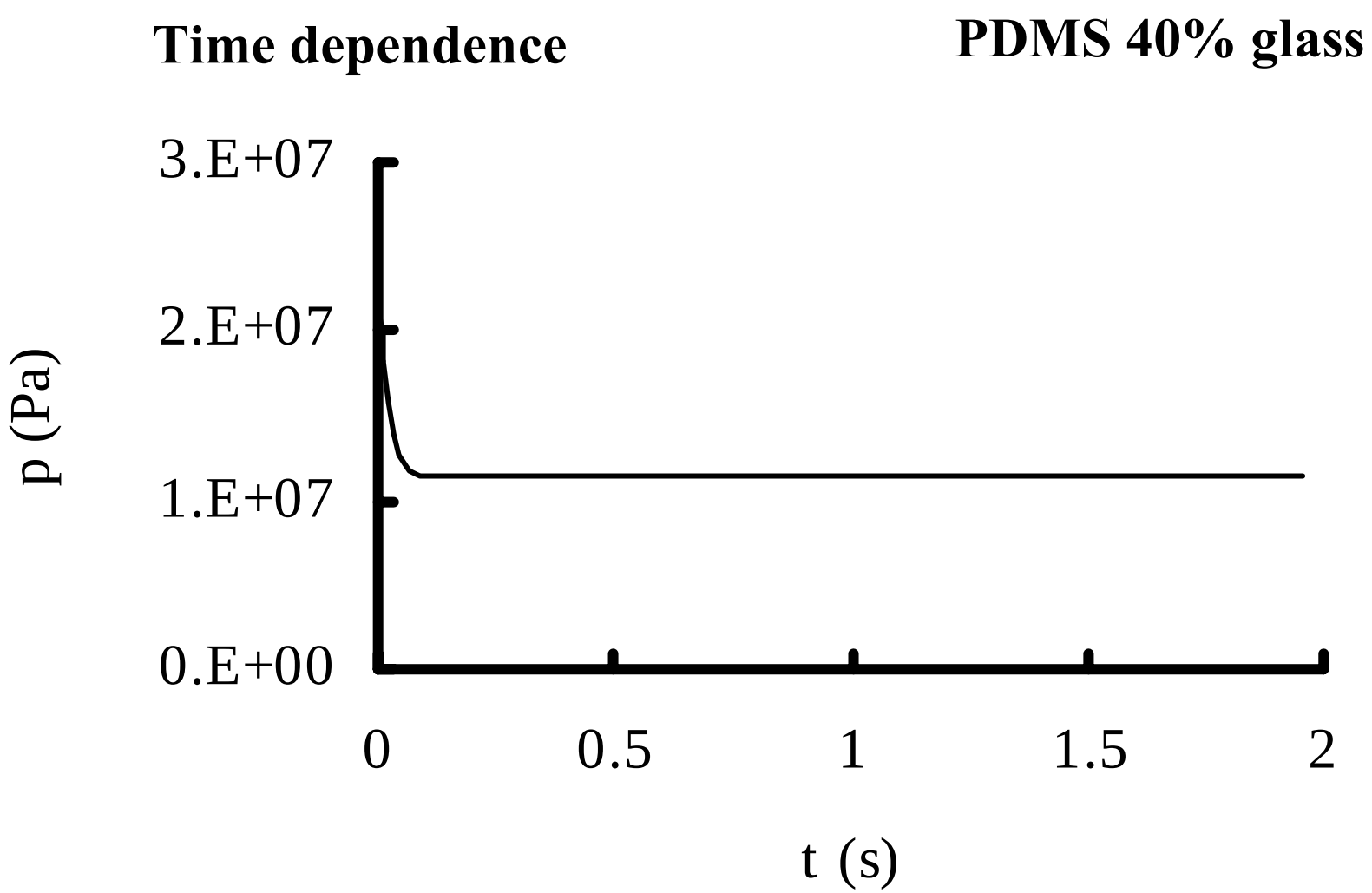

Solution for flow of PDMS suspension
2R=0.0015m, L/2R=40, V_0=0.01m/s.
In the figure, triangles represent slip velocity.

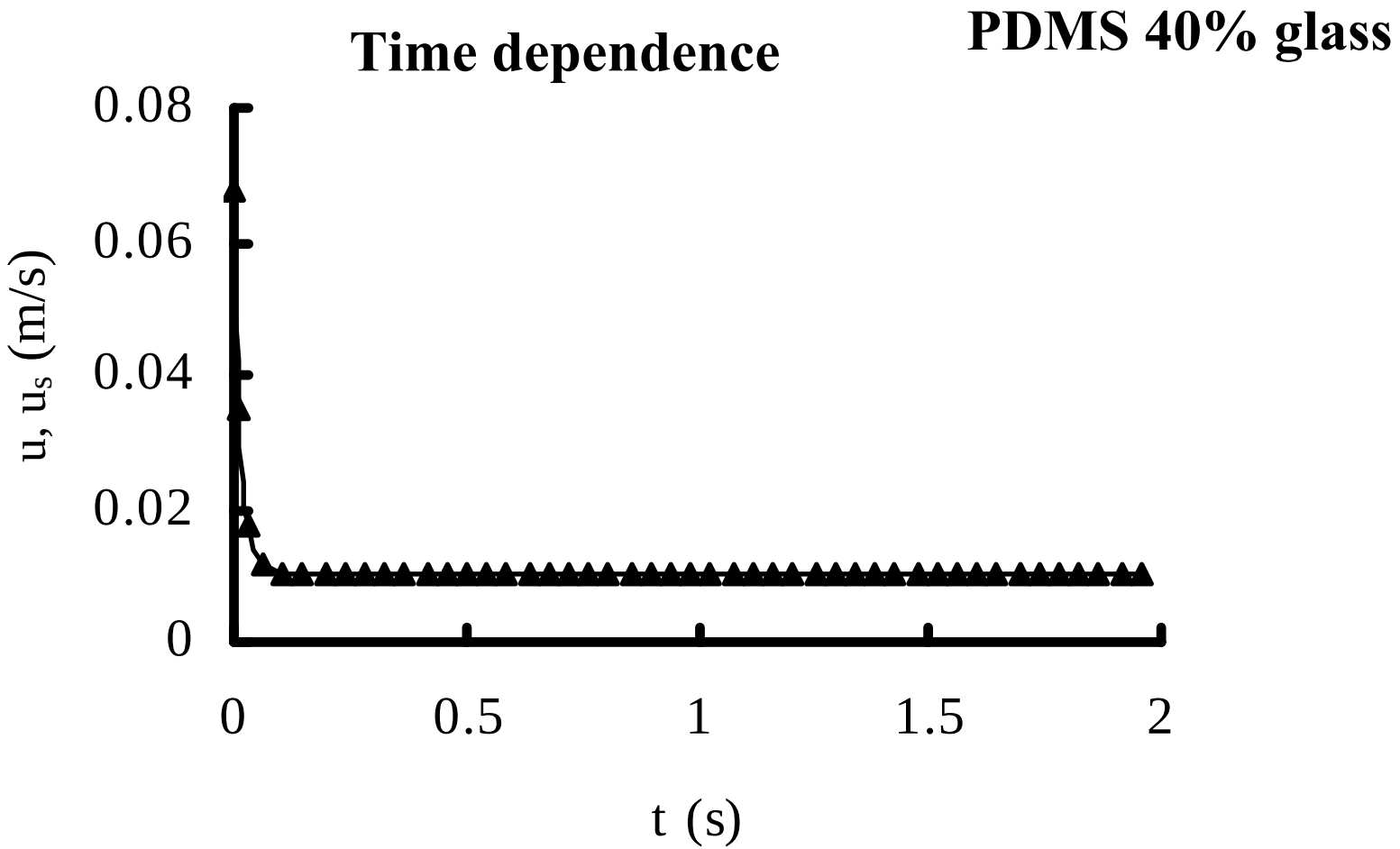

2R=0.0015m, L/2R=40, V_0=0.01m/s.
In the figure, triangles represent slip velocity.

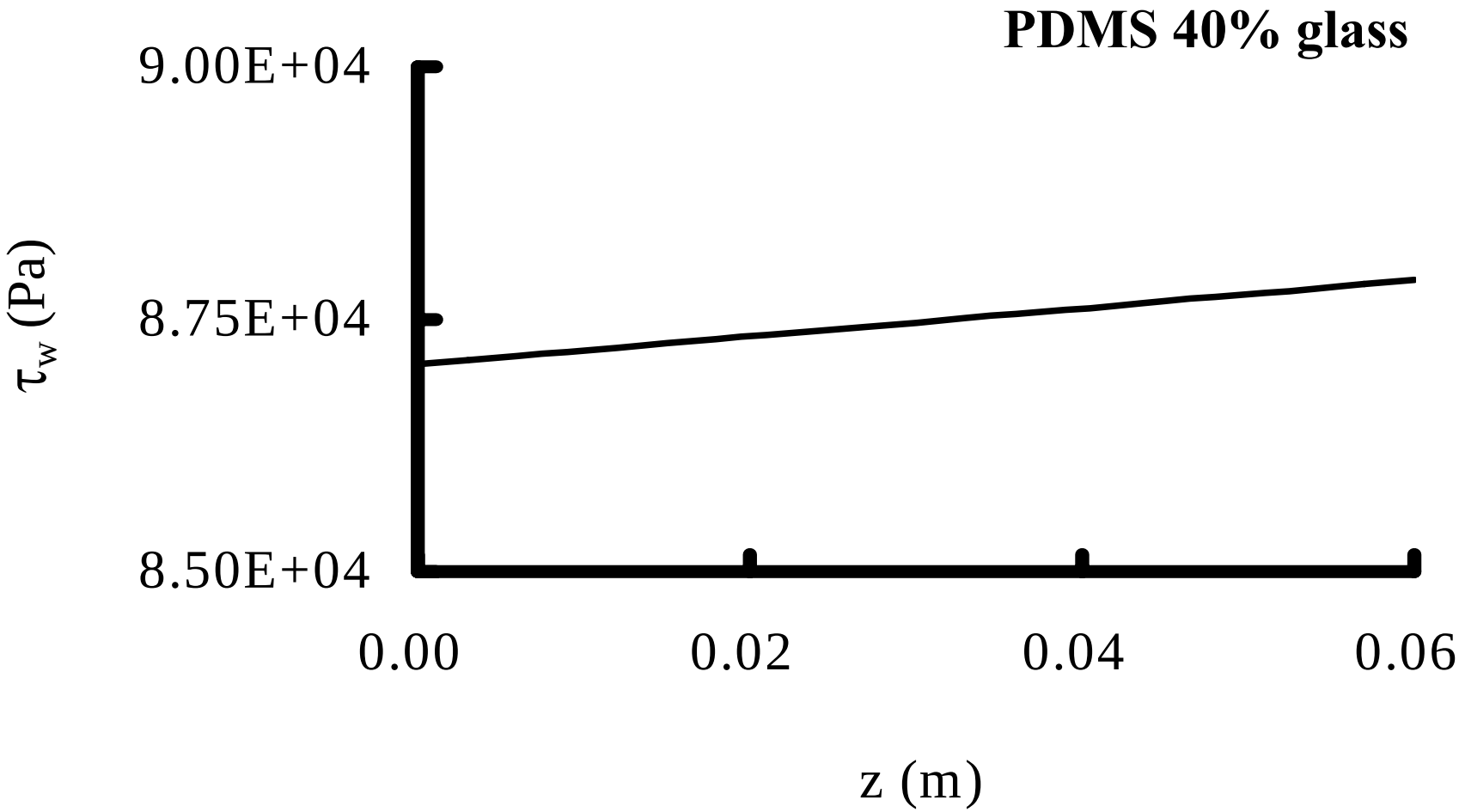

2R=0.0015m, L/2R=40, V_0=0.01m/s.
In the figure, triangles represent slip velocity.

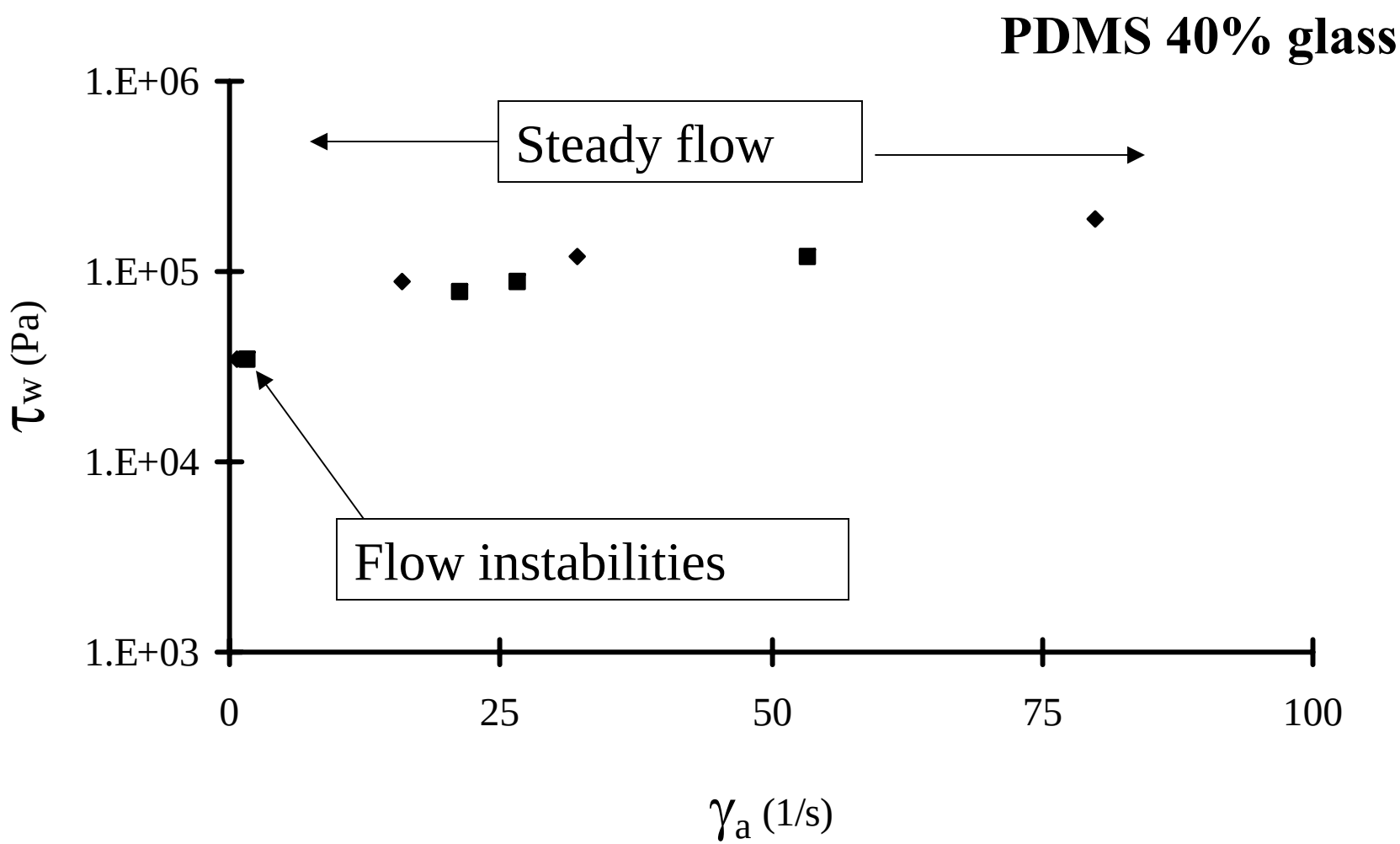

Filled symbols – prediction, hollow symbols—experiment.
Squares – 2R=0.0015m, L/2R=40, diamonds – 2R=0.0025m, L/2R=60.

Unfilled PDMS

Unfilled PDMS
(Slip velocity, Us, not pressure dependent):

$$u_s = \beta \tau_w^{sb} \left(1 + \tanh\left(\alpha(\tau_w - \tau_a)\right)\right)$$

Critical wall shear stress at which strong wall slip is observed: $\tau_a =$ **70,000 Pa**

$m = 17200 Pa \cdot s^{0.39}$, $n = 0.39$, $\tau_y = 0 Pa$,

$\beta_0 = 4.15 \times 10^{-15} \mathrm{m} \cdot \mathrm{s}^{-1} \cdot \mathrm{Pa}^{-2.26}$,

$\kappa = 0$, and $sb = 2.26$.

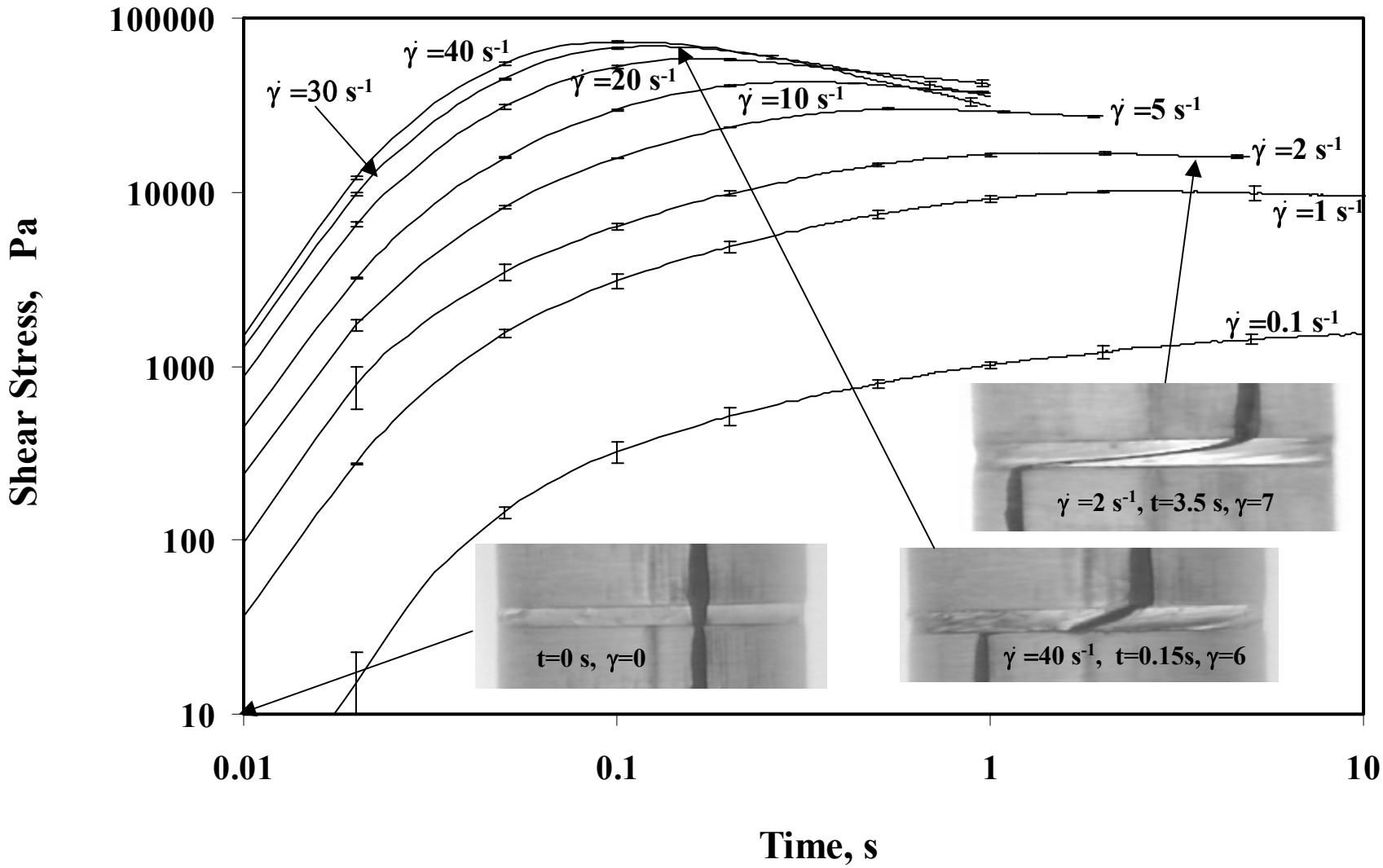

Steady torsional flow of poly(dimethyl siloxane) at various apparent shear rates and results of straight-line marker technique applied at the free surface of PDMS for detection of conditions under which wall slip is initiated.

Unfilled PDMS

$$u_s = \beta \tau_w^{sb} \left(1 + \tanh\left(\alpha(\tau_w - \tau_a)\right)\right)$$

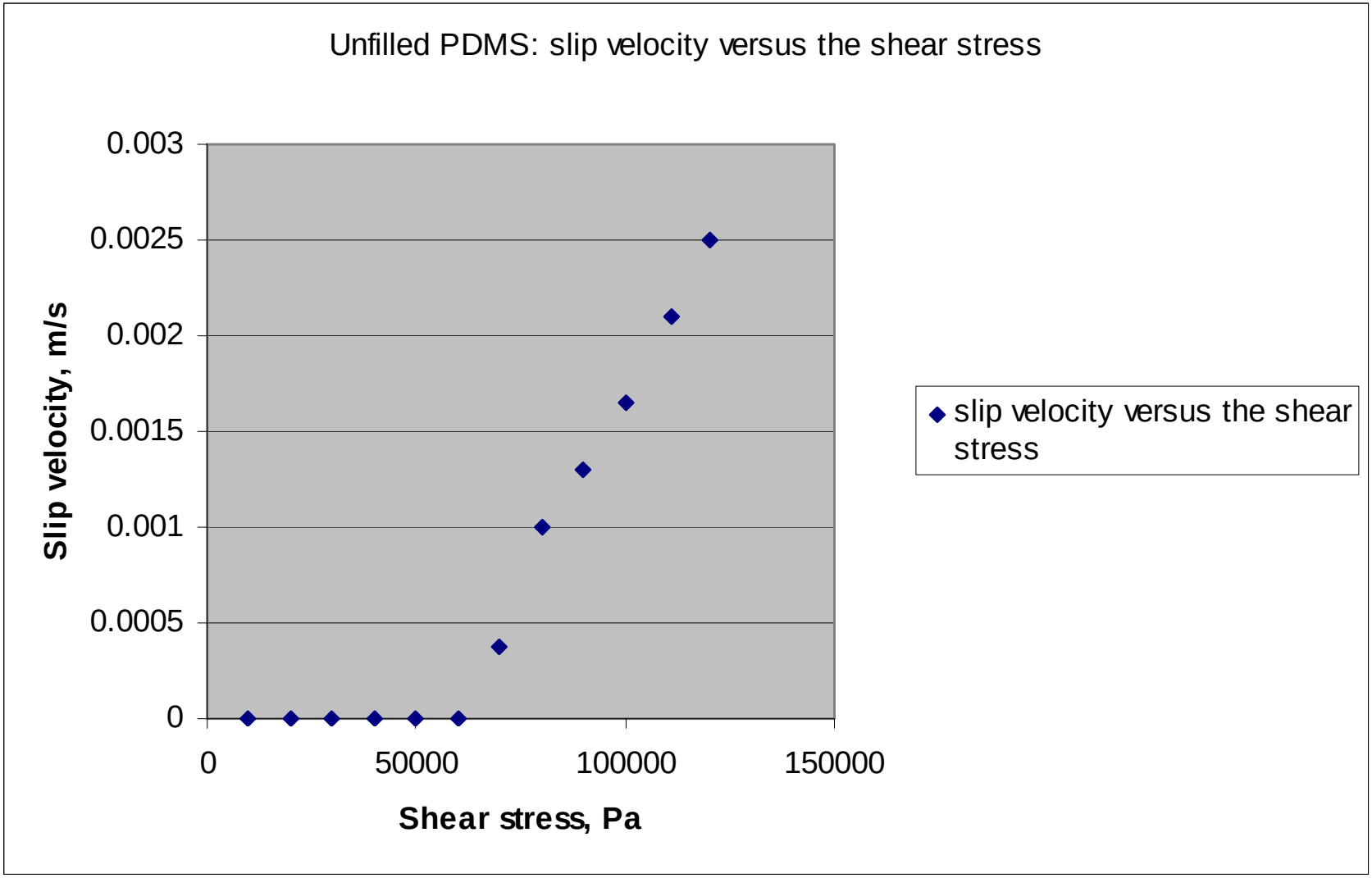

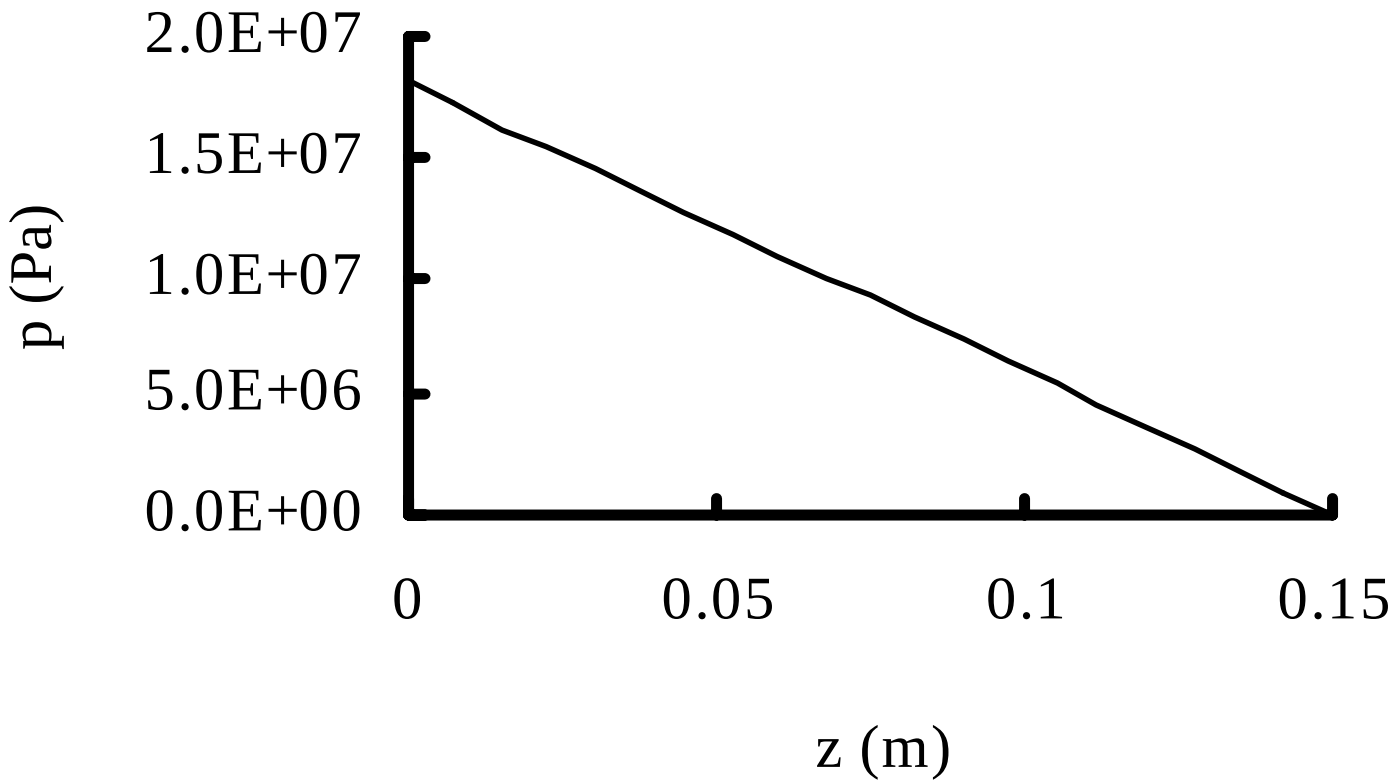

Unfilled PDMS:

2R=0.0025m, L/2R=60, V_0=0.001m/s.

In the figure, triangles represent slip velocity.

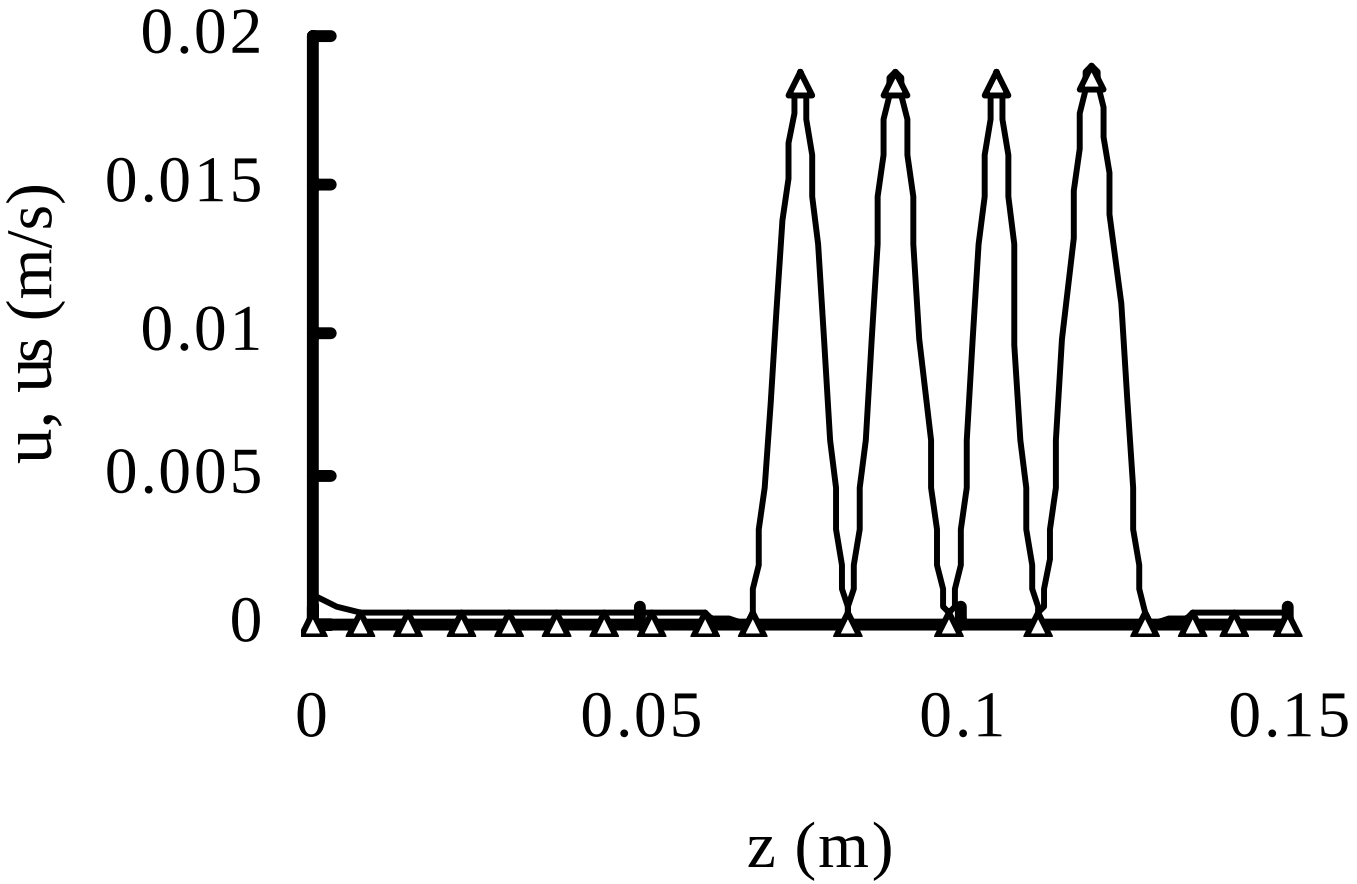

Unfilled PDMS:

2R=0.0025m, L/2R=60, V_0=0.001m/s.

In the figure, triangles represent slip velocity.

Distance dependence

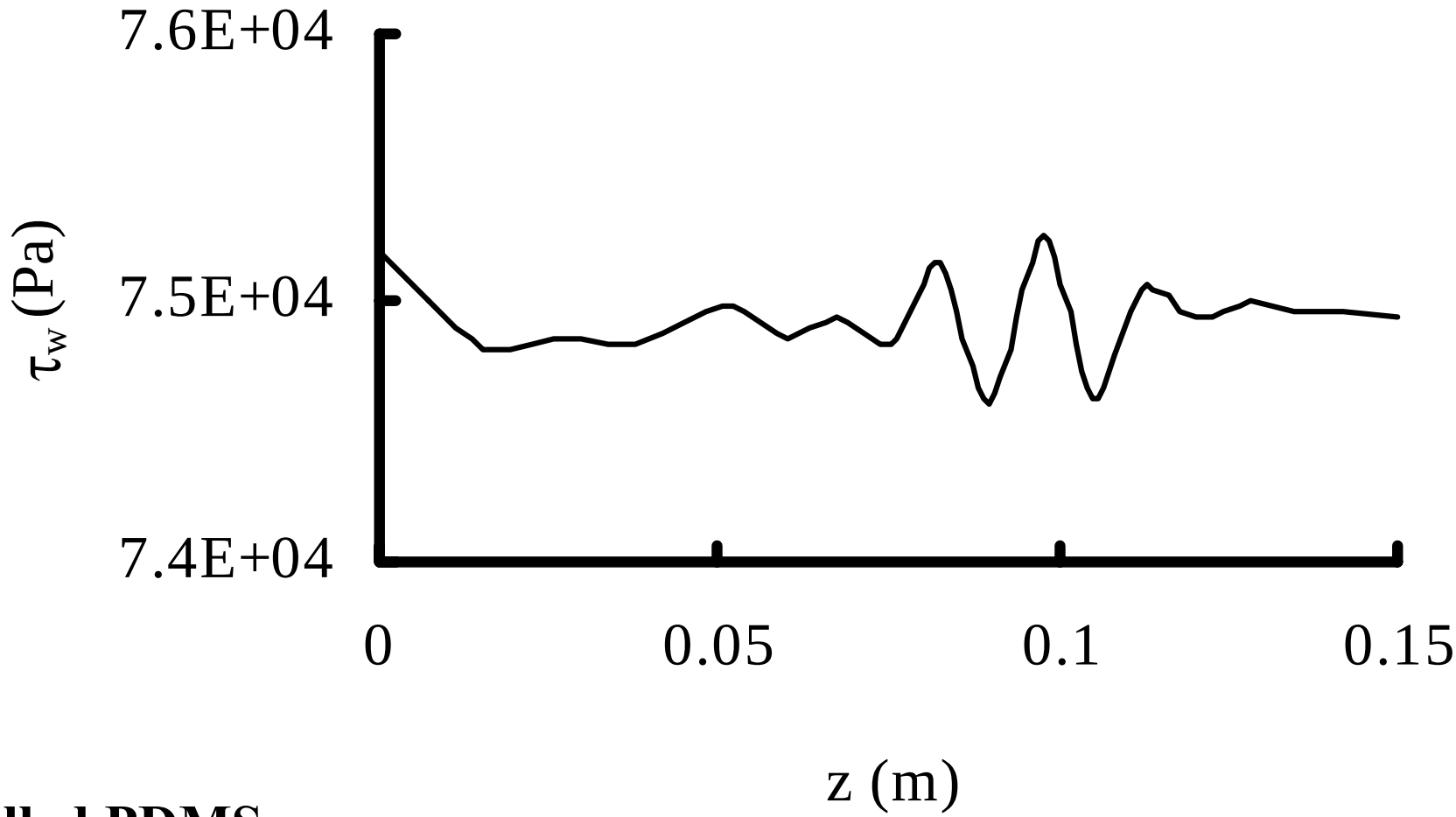

Unfilled PDMS:

2R=0.0025m, L/2R=60, V_0=0.001m/s.

In the figure, triangles represent slip velocity.

Time dependence

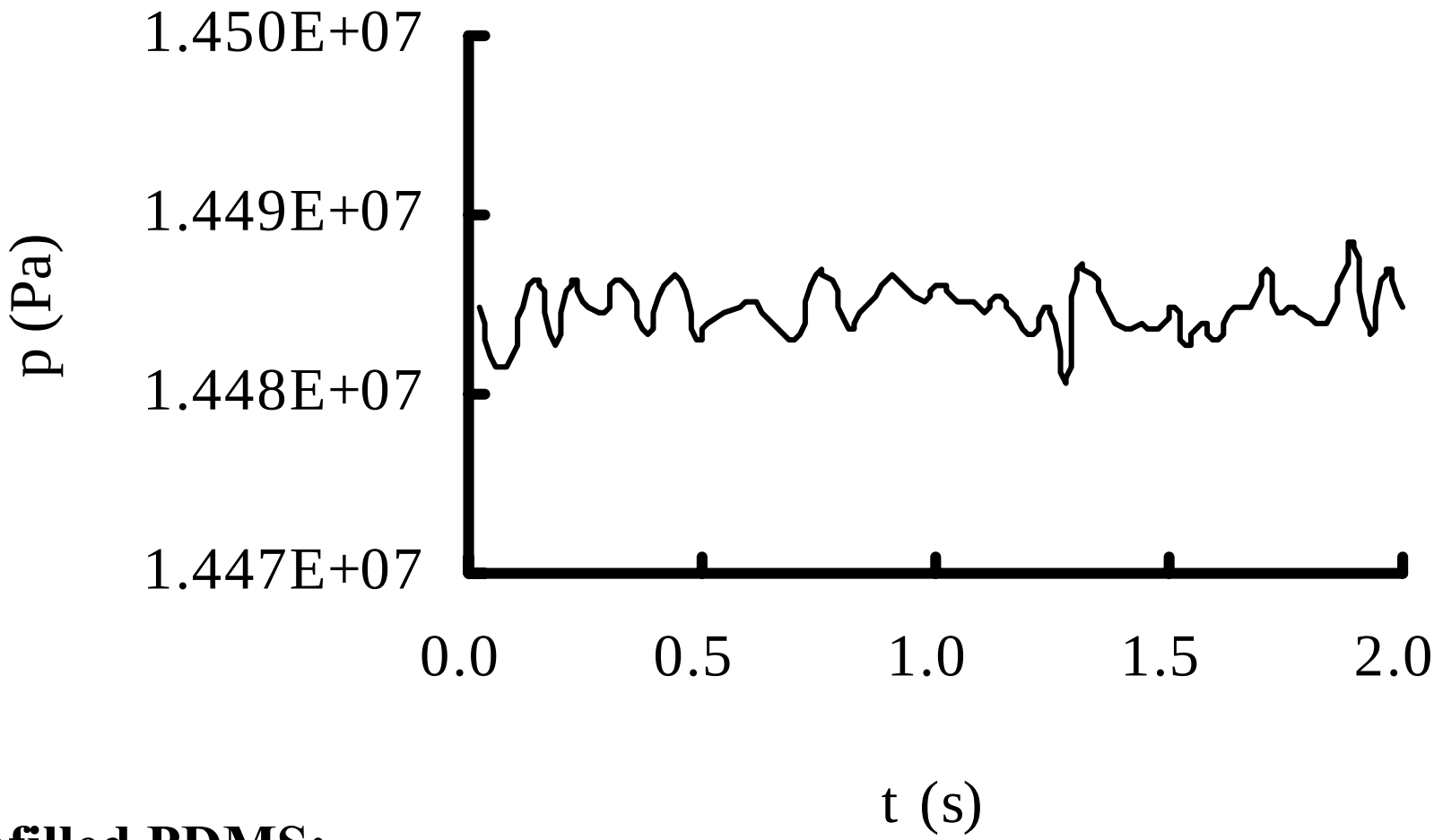

Unfilled PDMS:

2R=0.0025m, L/2R=60, V_0=0.001m/s.

In the figure, triangles represent slip velocity.

Time dependence

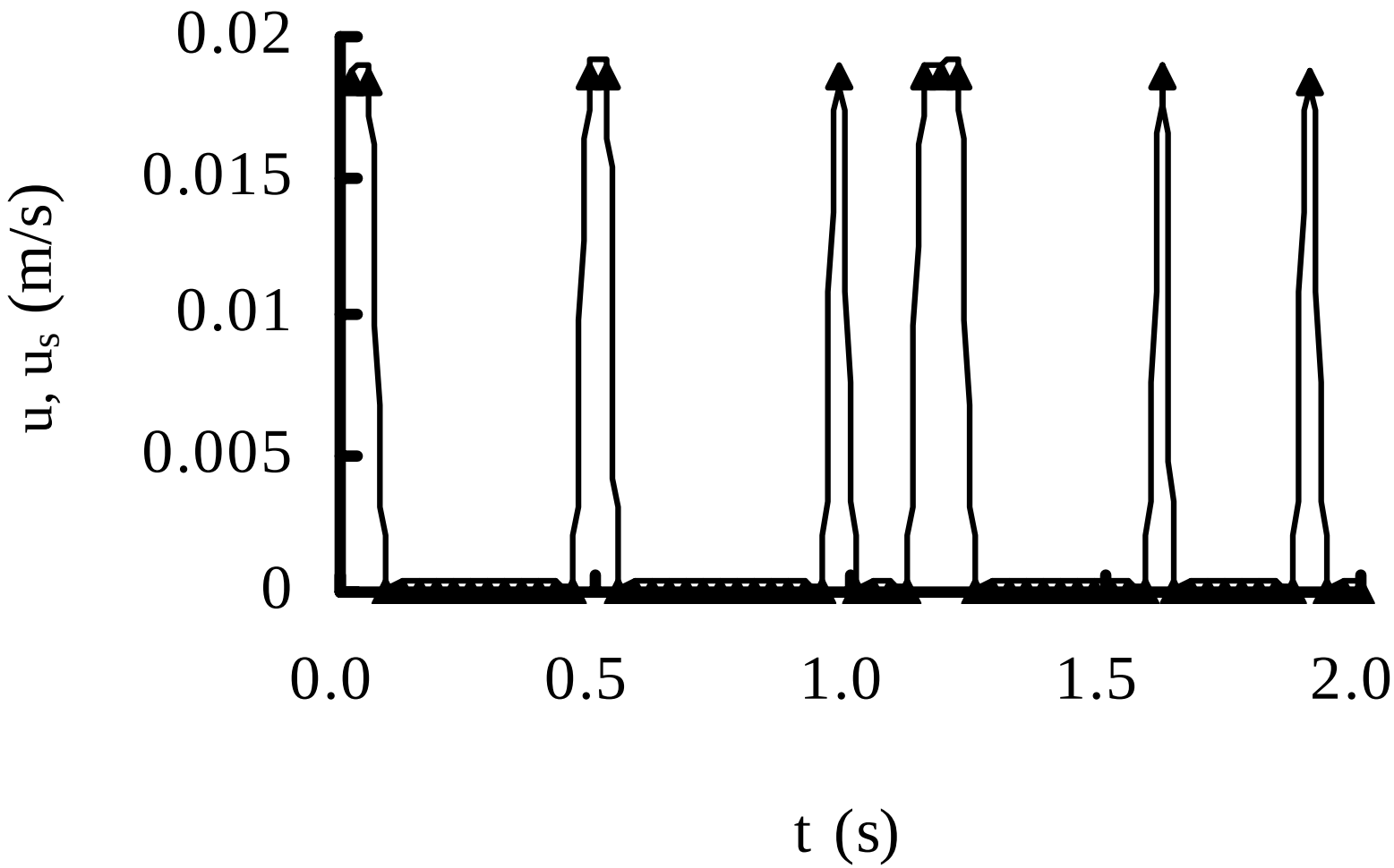

Unfilled PDMS:

2R=0.0025m, L/2R=60, V_0=0.001m/s.

In the figure, triangles represent slip velocity.

Conclusions

It appears that the stability of stick or slip at the wall during extrusion governs the occurrence of surface irregularities.

Conditions which give rise to wall shear stress values which are in the vicinity of the critical wall shear stress at which strong wall slip is onset give rise to flow instabilities.

Simulation provides the understanding necessary to predict the conditions under which flow instabilities form. Use the understanding to eliminate or minimize the formation of flow instabilities during processing of polymers and polymeric suspensions.